JAERI - M
82-166

ASSESSMENT OF TRAC-PD2 REFLOOD CORE THERMO-HYDRAULIC MODEL BY CCTF TEST C1-16

November 1982

Jun SUGIMOTO

日 本 原 子 力 研 究 所
Japan Atomic Energy Research Institute

JAERI-Mレポートは，日本原子力研究所が不定期に公刊している研究報告書です。
入手の問合わせは，日本原子力研究所技術情報部情報資料課（〒319-11茨城県那珂郡東海村）あて，お申しこみください。なお，このほかに財団法人原子力弘済会資料センター（〒319-11 茨城県那珂郡東海村日本原子力研究所内）で複写による実費頒布をおこなっております。

JAERI-M reports are issued irregularly.
Inquiries about availability of the reports should be addressed to Information Section Division of Technical Information, Japan Atomic Energy Research Institute, Tokai-mura, Naka-gun Ibaraki-ken 319-11, Japan.

編集兼発行　日本原子力研究所
印　　刷　(株)原子力資料サービス

JAERI-M 82-166

Assessment of TRAC-PD2 Reflood Core Thermo-hydraulic Model by CCTF Test C1-16

Jun SUGIMOTO

Division of Nuclear Safety Research,
Tokai Research Establishment, JAERI

(Received October 26, 1982)

The TRAC-PD2 reflood core thermo-hydraulic model was assessed by CCTF Test C1-16. The measured data were utilized as core boundary conditions in the TRAC calculations. The results indicate that the core inlet liquid temperature and the core heater rod temperatures are in reasonable agreement with data, but the pressure distribution in the core and water pool formation in the upper plenum are not in good agreement. The parametric effects of the droplet critical Weber number, the material properties of the heater rod, the noding of the upper plenum, and the minimum stable film boiling temperature are also discussed.

Keywords: LOCA, Reflood, TRAC Code, CCTF, Thermo-hydraulics, Two-phase flow, Heat Transfer.

The work was performed under contract with the Atomic Energy Bureau of Science and Technology of Japan.

JAERI－M 82－166

円筒炉心試験Ｃ１－16を用いたＴＲＡＣ－ＰＤ２の再冠水期炉心熱水力モデルの評価

日本原子力研究所東海研究所安全工学部
杉本　純

（１９８２年10月26日受理）

円筒炉心試験Ｃ１－16の結果を用いて，ＴＲＡＣ－ＰＤ２コードの再冠水期炉心熱水力モデルの評価を行った。ＴＲＡＣ－ＰＤ２による計算では実験で得られた値を炉心境界条件として与えた。解析の結果，炉心入口水温や発熱体温度挙動は実験と比較的良く一致したが，炉心内の圧力分布や上部プレナム蓄水挙動については良い一致は得られなかった。液滴の臨界ウェーバー数，発熱体の物性値，上部プレナムのノーディング，および最小安定膜沸騰温度についてパラメータ解析を行い，これらが炉心熱水力挙動に及ぼす影響を調べた。

本研究は，電源開発促進対策特別会計法に基づき，科学技術庁からの受託によって行われた。

Contents

目　　次

List of tables

List of figures

1. Introduction

The present work is an attempt to assess the core thermo-hydraulic model in TRAC-PD2[1] code for a reflood phase of a loss-of-coolant accident (LOCA) of a PWR. For this purpose, the experimental results of the Cylindrical Core Test Facility (CCTF) at Japan Atomic Energy Research Institute are compared with TRAC calculations.

The Transient Reactor Analysis Code (TRAC) is being developed at the Los Alamos National Laboratory to provide an advanced best-estimate predictive capability for the analysis of PWR LOCA. The code has two-phase nonequilibrium hydrodynamic models, the three-dimensional treatment capability of the pressure vessel, flow-regime-dependent constitutive equation treatment, and reflood tracking capability for both bottom and falling film quench fronts.

The CCTF has been designed to demonstrate the effectiveness of the emergency core cooling system, to verify the best-estimate analysis codes and to supply information for the improved thermo-hydraulic models during the reflood phase. The test facility is a 1/20 scale model with four primary loops of a 1000 MW PWR. The vertical dimensions are preserved to the reference PWR.

The bundle forced reflood experiments (FLECHT[2][3] and JAERI small reflood experiments[4][5]) have shown that the core heat transfer much depends on the core inlet mass velocity and also on the system pressure. The core inlet mass velocity, however, is expected to vary considerably in an actual reactor vessel, and a U-tube manometer flow oscillation could occur between the core and the downcomer during the reflood phase.

The reflood core thermo-hydraulic models in TRAC have been assessed against constant forced-feed FLECHT experiments[6]; however, the range of the inlet mass velocity is narrow compared with that of the gravity-feed system reflood experiments[7]. In a system calculation with TRAC[8], it is sometimes difficult to obtain a correct core inlet mass velocity unless the calculational behavior for all components throughout the system is correctly predicted. Therefore, it will be difficult to assess the core thermo-hydraulic models of TRAC in a system calculation. In the present calculation, only the core region was modeled in order to decouple the system feed-back effect, and the measured data were utilized as a core boundary condition.

The CCTF Test C1-16[9] was chosen for the present assessment,

because the ECC water was directly injected into the lower plenum and the downcomer wall was not heated above the saturation temperature in the test. This simple operational method allows a better estimation of the core inlet mass flow rate. The details of the CCTF facility and the experimental specifications of Test C1-17 are described in Ref. 9.

2. Description of the TRAC-PD2 model

The TRAC version used for the calculation was a released version of TRAC-PD2 (26.0)[1]. A modification was made in the core to model the material properties of the heater rod that are used in CCTF. The current version of PD2, however, cannot handle an axial variation of the heater rod materials, which is the case in CCTF.

The TRAC input model nodalization is shown in Fig. 1. The input model consisted of five components that are described in Table 1. The lower plenum, the lower plenum injection port, the core, and the upper plenum were modeled in the present calculation, but the four primary loops were omitted. The total number of computational fluid cells was 19.

A noding schematic of the vessel component is shown in Fig. 2. The downcomer region was also omitted for the purpose of the present analysis. TRAC automatically switches to a Cartesian coordinate system when a one-dimensional noding of the vessel is chosen, as in this modeling. The test vessel was subdivided into 13 axial levels, which allowed direct comparison to actual differential pressure measurements in the core. The coarse noding of the core region (six axial levels) required averaging of the CCTF axial power profile (17 axial levels), as shown in Fig. 3. It should be noted that the local power levels where thermocouples are located (elevations 3, 4, and 5 in Fig. 3) are almost identical with those of the experiment in the present noding.

The heater rod was segmented into nine radial nodes as shown in Fig. 4. The outer insulator is made of boron-nitride (BN) near the midplane and magnesium-oxide (MgO) at both ends of the heated length, as shown in Fig. 3. The effects of the material differences will be discussed in Sec. 4.2.

because the ECC water was directly injected into the lower plenum and the downcomer wall was not heated above the saturation temperature in the test. This simple operational method allows a better estimation of the core inlet mass flow rate. The details of the CCTF facility and the experimental specifications of Test C1-17 are described in Ref. 9.

2. Description of the TRAC-PD2 model

The TRAC version used for the calculation was a released version of TRAC-PD2 (26.0)[1]. A modification was made in the core to model the material properties of the heater rod that are used in CCTF. The current version of PD2, however, cannot handle an axial variation of the heater rod materials, which is the case in CCTF.

The TRAC input model nodalization is shown in Fig. 1. The input model consisted of five components that are described in Table 1. The lower plenum, the lower plenum injection port, the core, and the upper plenum were modeled in the present calculation, but the four primary loops were omitted. The total number of computational fluid cells was 19.

A noding schematic of the vessel component is shown in Fig. 2. The downcomer region was also omitted for the purpose of the present analysis. TRAC automatically switches to a Cartesian coordinate system when a one-dimensional noding of the vessel is chosen, as in this modeling. The test vessel was subdivided into 13 axial levels, which allowed direct comparison to actual differential pressure measurements in the core. The coarse noding of the core region (six axial levels) required averaging of the CCTF axial power profile (17 axial levels), as shown in Fig. 3. It should be noted that the local power levels where thermocouples are located (elevations 3, 4, and 5 in Fig. 3) are almost identical with those of the experiment in the present noding.

The heater rod was segmented into nine radial nodes as shown in Fig. 4. The outer insulator is made of boron-nitride (BN) near the midplane and magnesium-oxide (MgO) at both ends of the heated length, as shown in Fig. 3. The effects of the material differences will be discussed in Sec. 4.2.

3. Initial and boundary conditions

The initial test conditions used for the calculations are tabulated in Table 2. These test conditions and boundary conditions were taken from the experimental data.[9] The sequence of events is summarized in Table 3. All trips were made according to the actual sequence in the experiment. The characteristic features of the Test C1-16 experiment are that the system pressure is relatively high (0.41 MPa), the temperature of the emergency core cooling (ECC) water is relatively low (340 K) compared with the most base line tests of CCTF, and the direct lower plenum ECC injection mode is used for the FLECHT-coupling test.

The hydraulic boundary conditions for the TRAC calculation were specified so that the pressure in the upper plenum and the core inlet mass velocity agreed with the data. A time-dependent pressure table was specified for the break component, shown in Table 1, at the upper plenum. The liquid velocities and the liquid temperatures were specified for the fill components at the lower plenum (see Fig. 1). Figure 5 and 6 show the pressure in the upper plenum and the core inlet mass velocity used in the present analysis. The experimental data are shown as dotted lines. It should be noted that the core inlet mass velocity was evaluated considering the mass balance in the system, using differential pressure measurements in the core and upper plenum, and Pitot tube mass flow measurements in the cold legs.

4. Results and discussion

4.1 Base case calculation

Figure 7 shows the comparison of the measured and calculated core inlet liquid temperatures. Since the water temperature of the fill component in the lower plenum is set equal to 340 K and the calculation is in good agreement with the data, then the evaluated core inlet mass velocity, based on the mass balance calculation, must be in reasonable agreement with actual values.

Calculated heater rod temperature histories at five axial locations are compared with data in Figs. 8 through 12. This particular heater rod (28Z2 rod) was chosen for the comparison because it is located in

3. Initial and boundary conditions

The initial test conditions used for the calculations are tabulated in Table 2. These test conditions and boundary conditions were taken from the experimental data.[9] The sequence of events is summarized in Table 3. All trips were made according to the actual sequence in the experiment. The characteristic features of the Test C1-16 experiment are that the system pressure is relatively high (0.41 MPa), the temperature of the emergency core cooling (ECC) water is relatively low (340 K) compared with the most base line tests of CCTF, and the direct lower plenum ECC injection mode is used for the FLECHT-coupling test.

The hydraulic boundary conditions for the TRAC calculation were specified so that the pressure in the upper plenum and the core inlet mass velocity agreed with the data. A time-dependent pressure table was specified for the break component, shown in Table 1, at the upper plenum. The liquid velocities and the liquid temperatures were specified for the fill components at the lower plenum (see Fig. 1). Figure 5 and 6 show the pressure in the upper plenum and the core inlet mass velocity used in the present analysis. The experimental data are shown as dotted lines. It should be noted that the core inlet mass velocity was evaluated considering the mass balance in the system, using differential pressure measurements in the core and upper plenum, and Pitot tube mass flow measurements in the cold legs.

4. Results and discussion

4.1 Base case calculation

Figure 7 shows the comparison of the measured and calculated core inlet liquid temperatures. Since the water temperature of the fill component in the lower plenum is set equal to 340 K and the calculation is in good agreement with the data, then the evaluated core inlet mass velocity, based on the mass balance calculation, must be in reasonable agreement with actual values.

Calculated heater rod temperature histories at five axial locations are compared with data in Figs. 8 through 12. This particular heater rod (28Z2 rod) was chosen for the comparison because it is located in

the middle power zone, it has nearly the same local power (103 per cent) as input in TRAC when the core is assumed to have a flat radial power distribution, and finally it represents a typical temperature history when compared with other corresponding heater rods, as listed in Table 4. The heater rods chosen for the quench time evaluation are located in the central region of the middle power zone, as shown in Fig. 13. The calculations are in reasonable agreement with the data especially for the lower part of the core (see Figs. 8 and 9). TRAC tends to underpredict the quench time for the midplane and the upper part of the core (see Figs. 10 and 11). The spiky behavior shown in Fig. 12 indicates that the TRAC heat transfer is sensitive to the fluid conditions when a void fraction is high. TRAC tends to overpredict the quench temperature for the upper part of the core.

Differential pressures in the core are shown in Figs. 14 through 19. The TRAC predictions are generally in good agreement with the data for the lower region of the core, as shown in Figs. 14 through 16. However, TRAC tends to underpredict the differential pressures for the upper region of the core, as shown in Figs. 18 and 19. Also shown in the figure are the quench times when the quench front reached each pressure tap location of the differential pressure measurement. The close comparison of the data with the calculation shows that TRAC slightly underpredicts the differential pressure below the quench front and overpredicts it above the quench front. This means that the calculated void fraction above the quench front is higher than the experiment. In the CCTF experiment, a fairly large amount of water accumulation was observed in the upper part of the core just after the reflood initiation as shown in Figs. 18 and 19. This implies that the slug flow rather than the dispersed flow has been established along the whole core at an early reflood transient.

The differential pressure in the upper plenum is shown in Fig. 20. The calculation shows very little water accumulation in the upper plenum, whereas the data show significant water formation due to carry-over from the core and de-entrainment in the upper plenum. Figure 21 shows the calculated core outlet liquid mass velocity. TRAC predicts a periodic outlet liquid mass velocity (carry-over water), but it does not predict the water pool formation in the upper plenum. This is because TRAC currently does not have a de-entrainment model based on a droplet field.

Figure 22 shows the liquid mass in the core. The data was evaluated

from the differential pressure measurement across the core. Although the detailed differential pressure distribution shown in Figs. 14 through 19 does not precisely agree well with each other, the summed core liquid mass is in reasonable agreement with the data. According to the mass balance in the core, this indicates that the carry-over water was calculated reasonably on an average basis. However, the calculated carry-over water at each instant of time is not always reasonable, as shown in Fig. 21.

The base case calculation described above generally shows reasonable agreement with data, except for the pressure distribution in the core and the water pool formation in the upper plenum. Since the void fraction, and hence the liquid accumulation above the quench front affects the heat transfer, it is necessary to improve the hydraulic model to predict the pressure distribution in the core. It is considered that the water pool formation in the upper plenum may affect the top-down quenching phenomenon, due to the "fall-back" effect. On the other hand, the core inlet mass flow rate is the sum of 1) the water mass accumulation rate in the core, 2) the water mass accumulation rate in the upper plenum and 3) the loop mass flow rate. Therefore, it is important to correctly predict the water accumulation in the upper plenum to predict the top-down quenching and also the core inlet mass flow rate in the case of the system calculation.

The input listing for the base case calculation is contained in the Appendix.

4.2 Parametric calculations

4.2.1 Critical Weber number

In the transition boiling flow regime in TRAC-PD2,[1] the fraction of the liquid entrainment E is determined as,

$$E = \begin{cases} 0 & (|V_g| \leq V_E) \\ 1 - \exp\{0.23[-(|V_g| - V_E)]\} & (|V_g| > V_E) \end{cases} , \qquad (1)$$

where V_g is the vapor velocity and the entrainment velocity V_E is given by the critical Weber number Wec:

$$V_E = 2.33\left[\frac{(\rho_\ell - \rho_g)\mathrm{Wec}\ \sigma}{\rho_g^2}\right]^{0.25}, \qquad (2)$$

where ρ_ℓ and ρ_g denote the liquid and vapor density, respectively, and σ is the surface tension of the droplet.

The ceritical Weber number, which determines the diameter of the water droplet, is currently set to 4.0 in TRAC-PD2. Since it is sensitive to the water carry-over phenomena and also to the heat transfer above the quench front[10], the parametric study of the critical Weber number was performed.

The effect of the droplet critical Weber number on the quench front propagation is shown in Fig. 23. As shown in the figure, the quench envelope generally agrees well with the data for the case of Wec = 1.0, especially for the lower half of the core below 1.83 m elevation, however, good agreement was not obtained for the top part of the core due to the poor pre-cooling and the oscillatory behavior of the temperaure as shown in Fig. 12.

Top-down quenching and large variations in the quench times are observed only for the top part of the core in the experiment. This is due to the fall-back effect caused by the water pool formation in the upper plenum. It appears to depend on the type of upper plenum structure above the thermocouple location. The internals consist of control rod guide tubes, stub mixers, open holes, support columns with mixers, and orifice plates. There is a tendency for the thermocouples below the stub mixers to show later quenching and the ones below the open holes to show earlier quenching, as shown in Fig. 24. However, this wide spread of the quench time is only observed above 3.05 m elevation from the bottom of the core, and the quench front moves nearly one-dimensionally in the rest of the core as shown in Fig. 23.

The core liquid mass are compared in Fig. 25. Since the larger critical Weber number generally results in less carry-over, the case of We = 4.0 yields better agreement with the data than any other. However, it should be noted that the calculation of carry-over water in TRAC = PD2 is not a very stable process as indicated in Fig. 21, and needs improvement.

4.2.2 Material properties of the heater rod

Figure 26 shows the effect of material properties of the heater rod on the temperature response. As shown in Figs. 3 and 4, boron-nitride (BN) is used as an insulator between the cladding and the heater element near the midplane, and magnesium-oxide (MgO) is used for both ends of the heated length. Although the thermal conductivity of boron-nitride is several times larger than that of magnesium-oxide, the temperature responses of the two are quite similar. This indicates that the difference of the material properties of the heater rod used in CCTF does not much affect the reflood thermal behaviors. This is because that the reflood process proceeds at a rate which is much longer than the time constant of either type of heater rod.

4.2.3 Upper plenum noding

In the upper plenum noding of the base case, two major flow area changes were modeled at the tie plate (5.76 m) and at the upper core support plate (6.117 m). The top part noding was made to maintain the proper elevation of the hot leg. In CCTF, however, there exist rather unobstructed flow areas between the two paltes and also above the short columns elevation. Therefore the parametric calculation was performed to investigate the effect of the upper plenum noding on the de-entrainment phenomena observed in the experiment. Figure 27 shows the noding diagram used for these calculations. The number of cells in the upper plenum N(UP) was three for the base case calculation.

Figure 28 shows the effect of the upper plenum noding on the water pool formation. A small amount of water accumulation was calculated for the case of N(UP) = 4 (after 230 s); however, no significant water accumulation compared with the data was calculated. This means it may be necessary for TRAC to have some kind of upper plenum de-entrainment model based on the experimental results.

4.2.4 Minimum stable film boiling temperature

The minimum stable film boiling point is the intersection between the transition and the film boiling heat-transfer regimes in the TRAC-PD2 boiling curve. This correlation is given by[11]

$$T_{min} = T_{hn} + (T_{hn} - T_{\ell}) \left[\frac{k_{\ell}\rho_{\ell}C_{p\ell}}{k_{w}\rho_{w}C_{pw}}\right]^{\frac{1}{2}} , \quad (3)$$

where T_{min} is the minimum stable film boiling temperature, T_{hn} is the homogeneous nucleation temperature, and subscripts ℓ and w denote liquid and wall, respectively.

T_{hn} is a weak function of pressure, varying from 580 K at atmospheric pressure to the critical temperature (647.3 K). IN TRAC-PD2, however, the pressure dependence of T_{hn} was not modeled and was set equal to 647.3 K. A run was made with a functional relationship between T_{hn} and pressure by a simple curve fit,

$$T_{hn} = 705.44 - 4.722 \times 10^{-2} \cdot (3203.6 - P) + 2.3907 \times 10^{-5} \cdot (3203.6-P)^2 - 5.8193 \times 10^{-9} \cdot (3203.6 - P)^3 \quad (4)$$

where T_{hn} is in °F and the pressure P in psia.

The effects of the T_{min} correlation as a function of pressure on the heater rod temprerature are shown in Figs. 29 through 33. It is shown that the overall temperature histories, especially the quench time and the quench temperature, are much better predicted for the case of the T_{min} correlation corrected for the pressure dependence. This is because the T_{min} correlation with Eq. (4) gives lower minimum stable film boiling temperature than the base case calculation under the system pressure (0.41 MPa) condition (about 50 K lower), resulting in the slower quench front propagation in the upper part of the core. Although the investigation of the T_{min} correlation for much lower system pressure experiments of CCTF may be necessary, its use would be highly recommended based on the present analysis.

5. Conclusions

The assessmental calculation of TRAC-PD2 reflood heat transfer was performed using the measured core boundary conditions of CCTF Test C1-16. The following conclusions were obtained by comparing the calculation with the experiment.

1. The calculated core inlet liquid temperature is in good agreement with the data, which shows the validity of the present assessmental calculation method concerning the core inlet flow condition.

$$T_{min} = T_{hn} + (T_{hn} - T_{\ell}) \left[\frac{k_{\ell}\rho_{\ell}C_{p\ell}}{k_{w}\rho_{w}C_{pw}}\right]^{\frac{1}{2}} , \quad (3)$$

where T_{min} is the minimum stable film boiling temperature, T_{hn} is the homogeneous nucleation temperature, and subscripts ℓ and w denote liquid and wall, respectively.

T_{hn} is a weak function of pressure, varying from 580 K at atmospheric pressure to the critical temperature (647.3 K). IN TRAC-PD2, however, the pressure dependence of T_{hn} was not modeled and was set equal to 647.3 K. A run was made with a functional relationship between T_{hn} and pressure by a simple curve fit,

$$T_{hn} = 705.44 - 4.722 \times 10^{-2} \cdot (3203.6 - P) + 2.3907 \times 10^{-5} \cdot (3203.6-P)^2 - 5.8193 \times 10^{-9} \cdot (3203.6 - P)^3 \quad (4)$$

where T_{hn} is in °F and the pressure P in psia.

The effects of the T_{min} correlation as a function of pressure on the heater rod temprerature are shown in Figs. 29 through 33. It is shown that the overall temperature histories, especially the quench time and the quench temperature, are much better predicted for the case of the T_{min} correlation corrected for the pressure dependence. This is because the T_{min} correlation with Eq. (4) gives lower minimum stable film boiling temperature than the base case calculation under the system pressure (0.41 MPa) condition (about 50 K lower), resulting in the slower quench front propagation in the upper part of the core. Although the investigation of the T_{min} correlation for much lower system pressure experiments of CCTF may be necessary, its use would be highly recommended based on the present analysis.

5. Conclusions

The assessmental calculation of TRAC-PD2 reflood heat transfer was performed using the measured core boundary conditions of CCTF Test C1-16. The following conclusions were obtained by comparing the calculation with the experiment.

1. The calculated core inlet liquid temperature is in good agreement with the data, which shows the validity of the present assessmental calculation method concerning the core inlet flow condition.

2. The calculated heater rod temperature histories are in reasonable agreement with the data, however, TRAC generally tends to underpredict the quench time and to overpredict the quench temperature.
3. The calculated core differential pressures are in good agreement for the lower region of the core, but in poor agreement for the upper region. This is due to the overprediction of the void fraction above the quench front. The flow above the quench front is considered to be the slug flow in CCTF.
4. The critical Weber number of the water droplet used in TRAC was found to be sensitive to the liquid carry-over and to the core cooling. It is considered that the proper critical Weber number is in the range of 1.0 to 4.0.
5. TRAC shows that the difference in the heater rod materials (BN and MgO) that are used in CCTF has little effect on the experimental results because of the relatively slow reflood transient.
6. TRAC does not predict the water accumulation in the upper plenum as compared with the data for the number of levels in the upper plenum tested in the present study, probably due to the lack of the de-entrainment model in the upper plenum.
7. The use of the minimum stable film boiling temperature correlation as a function of pressure is recommended for reflood heat transfer calculations to better predict the quench time and the quench temperature.

Acknowledgements

This work was performed during the stay at Los Alamos National Laboratory (LANL) where the author was delegated as a resident engineer in the 2D/3D program since March 1980 to March 1981. He is much indebted to Dr. W. Kirchner, Messrs. K. Williams, R. Fujita, and T. Brown of LANL for their helpful advice and valuable discussions, and several helpful discussions with the members of LANL are gratefully acknowledged. He is grateful to Dr. M. Nozawa, director of the Nuclear Safety Research Center, to Dr. S. Katsuragi, head of Div. of Nuclear Safety Research, to Dr. M. Ishikawa, deputy head of Div. of Nuclear Safety Research and to Dr. K. Hirano, Chief, Reactor Safety Laboratory II at JAERI for their guidance and encouragement. Grateful appreciation is also expressed to Dr. Y. Murao, Dr. H. Akimoto and to the members of the Reactor Safety Laboratory II, for their help and advice.

2. The calculated heater rod temperature histories are in reasonable agreement with the data, however, TRAC generally tends to underpredict the quench time and to overpredict the quench temperature.
3. The calculated core differential pressures are in good agreement for the lower region of the core, but in poor agreement for the upper region. This is due to the overprediction of the void fraction above the quench front. The flow above the quench front is considered to be the slug flow in CCTF.
4. The critical Weber number of the water droplet used in TRAC was found to be sensitive to the liquid carry-over and to the core cooling. It is considered that the proper critical Weber number is in the range of 1.0 to 4.0.
5. TRAC shows that the difference in the heater rod materials (BN and MgO) that are used in CCTF has little effect on the experimental results because of the relatively slow reflood transient.
6. TRAC does not predict the water accumulation in the upper plenum as compared with the data for the number of levels in the upper plenum tested in the present study, probably due to the lack of the de-entrainment model in the upper plenum.
7. The use of the minimum stable film boiling temperature correlation as a function of pressure is recommended for reflood heat transfer calculations to better predict the quench time and the quench temperature.

Acknowledgements

This work was performed during the stay at Los Alamos National Laboratory (LANL) where the author was delegated as a resident engineer in the 2D/3D program since March 1980 to March 1981. He is much indebted to Dr. W. Kirchner, Messrs. K. Williams, R. Fujita, and T. Brown of LANL for their helpful advice and valuable discussions, and several helpful discussions with the members of LANL are gratefully acknowledged. He is grateful to Dr. M. Nozawa, director of the Nuclear Safety Research Center, to Dr. S. Katsuragi, head of Div. of Nuclear Safety Research, to Dr. M. Ishikawa, deputy head of Div. of Nuclear Safety Research and to Dr. K. Hirano, Chief, Reactor Safety Laboratory II at JAERI for their guidance and encouragement. Grateful appreciation is also expressed to Dr. Y. Murao, Dr. H. Akimoto and to the members of the Reactor Safety Laboratory II, for their help and advice.

References

(1) Liles, D., et al., "TRAC-PD2, An Advanced Best-Estimate Computer Program for Pressurized Water Reactor Loss-of-Coolant Accident Analysis," Los Alamos National Laboratory report LA-8709-MS, NUREG/CR-2054, April (1981).

(2) Murao, Y., et al., "Report on Series 5 Reflood Experiment," JAERI-M7383, in Japanese (October 1977).

(3) Sugimoto, J., et al., "Data Report on Reflood Experiment VIII (Series 6, Heat Transfer Data)," JAERI-M 8169, in Japanese (March 1979).

(4) Rosal, E.R., et al., "FLECHT Low Flooding Rate Cosine Test Series Data Report," Westinghouse Electric Corporation report WCAP-8651 (1975).

(5) Lilly, G.P., et al., "PWR-FLECHT Cosine Low Flooding Rate Test Series Evaluation Report, "Westinghouse Electric Corporation report WCAP-8838 (1977).

(6) Vigil, J.C., et al., "TRAC-PIA Developmental Assessment, "Los Alamos Scientific Laboratory report LA-8056-MS, NUREG/CR-1059 (October 1979).

(7) Waring, J.P., and Hochreiter, L.E., "PWR-FLECHT-SET Phase B1 Evaluation Report," Westinghouse Electric Corporation report WCAP-8583 (1975).

(8) Sugimoto, J., "TRAC-PD2 Posttest Analysis of CCTF Test C1-16 (RUN 025)," Los Alamos National Laboratory report LA-8741-MS, NUREG/CR-1991, May (1981).

(9) Murao, Y., and Sudoh, T., "Evaluation Report on CCTF-Core I Reflood Tests C1-16 (RUN 25), C1-21 (RUN 40) and C1-22 (RUN 41)," JAERI-M (to be published).

(10) Forslund, R.P. and Rohsenow, W.M, "Dispersed Flow Film Boiling," J. Heat Trans. 90 399-407 (1968).

(11) Henry, R.E., "A correlation for the Minimum Film Boiling Temperature," AICHE Symposium Series 138, 81-90 (1974).

Table 1 Component description

Component Number	Component Type	Description	Cells
1	FILL	ECC injection port	1
2	VALVE	Lower plenum injection nozzle	3
3	PIPE	Exhaust hot legs	1
4	BREAK	Upper plenum back pressure	1
5	VESSEL	13 axial levels; lower plenum levels 5 through 10, upper plenum levels 11 through 13, piping connections in levels 2 and 12	13

Table 3 Sequence of events for Test C1-16

Event	Measured (s)	Calculated (s)
Test initiated (heater rod power turned on)	0.0	0.0
Accumulator injection initiated (lower plenum)	49.0	49.0
Power decay initiated (Bottom of core recovery)	58.0	58.0
Time to reach peak rod surface temperature at core midplane (TE28Z23)	68.0	71.0
Accumulator injection ended and LPCI initiated (lower plenum)	75.0	75.0
Midplane of the heater rod quenched (TE28Z23)	161.5	133.5
All heater rods quenched	268.0	262.0

Table 2 Initial conditions for Test C1-16

	Measured
Power	
Total (MW)	9.28
Linear (kW/m)	1.5
Radial power distribution	1.06:1.0:0.79
Decay type	1.2 × ANS + Actinide
Pressure (Pa)	
System	4.1×10^5
Steam generator secondary	5.0×10^6
Temperature (K)	
Downcomer wall	410.2
Primary piping wall	418.2
Steam generator secondary	536.2
Peak clad at ECC initiation	801.2[a]
Peak clad at BOCREC	866.2[a]
Lower plenum filled liquid	400.2
ECC liquid	340.2
Water Level (m)	
Lower plenum	0.9
Steam generator secondary	7.4
ECC Injection Rate (m^3/s)	
Accumulator	0.100
LPCI	0.011

[a] Measured at highest power rod in highest power region.

Table 4 Summary of quench times for Test C1-16

		Symbol (Elevation: m)				
Bundle	Rod	1(0.38)	2(1.015)	3(1.83)	4(2.44)	5(3.05)
18	Z1	59.0	82.5	161.0	213.5	244.0
19	Z1	59.0	81.0	154.5	203.0	198.5
21	Z1	59.0	82.5	165.5	220.0	109.5
22	Z1	59.0	83.0	170.5	221.0	214.0
22	Z2	59.0	84.0	168.0	219.5	112.5
24	Z1	59.0	81.0	166.5	221.5	251.5
25	Z1	59.0	82.5	163.5	215.5	172.5
27	Z1	59.0	82.5	163.5	214.0	209.0
28	Z1	59.0	81.5	167.0	221.5	221.5
28	Z2	59.0	82.5	161.5	210.5	184.5
Average		59.0	82.3	164.2	216.0	191.8
σ_{n-1}		0	0.9	4.5	6.0	48.9
Bundle	Rod	1(0.289)	2(0.639)	3(0.889)	4(1.139)	5(1.454)
26	Z5	58.5	62.5	74.5	93.5	127.5
32	Z5	58.5	63.0	73.5	92.0	128.5
Average		58.5	62.8	74.0	92.8	128.0
Bundle	Rod	1(1.769)	2(2.089)	3(2.719)	4(3.289)	5(3.539)
26	Z6	165.0	192.5	-	72.0	66.0
32	Z6	168.5	187.0	98.5	71.0	66.5
Average		166.8	189.8	98.5	71.5	66.3

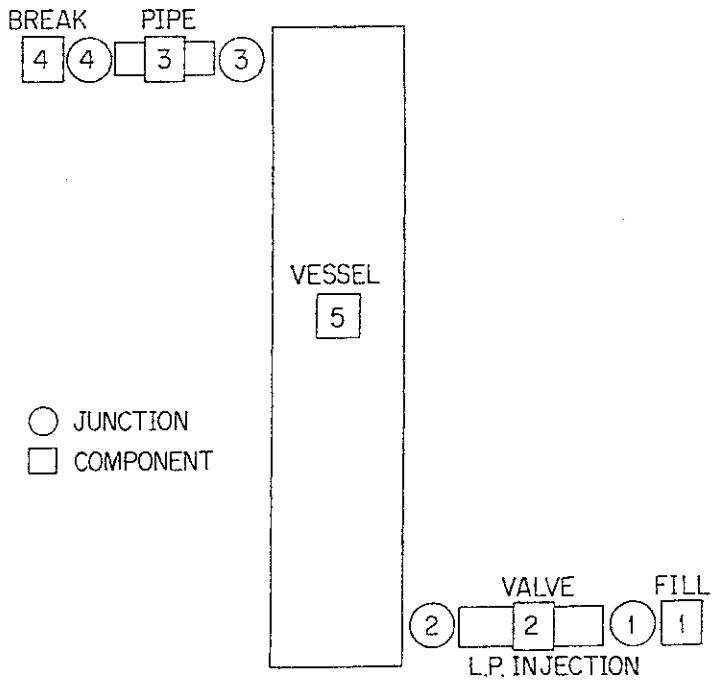

Fig. 1 TRAC schematic for CCTF core assessment

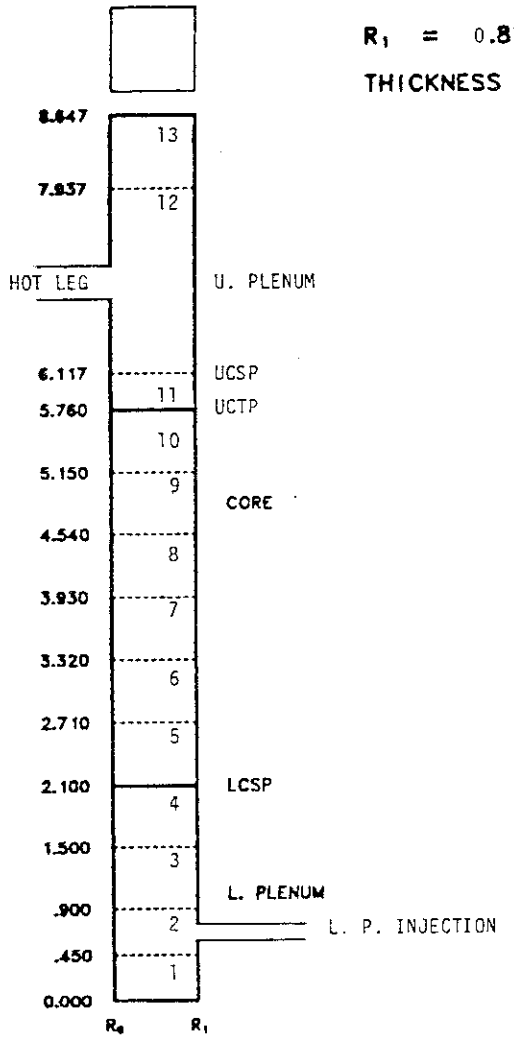

Fig. 2 Vessel noding

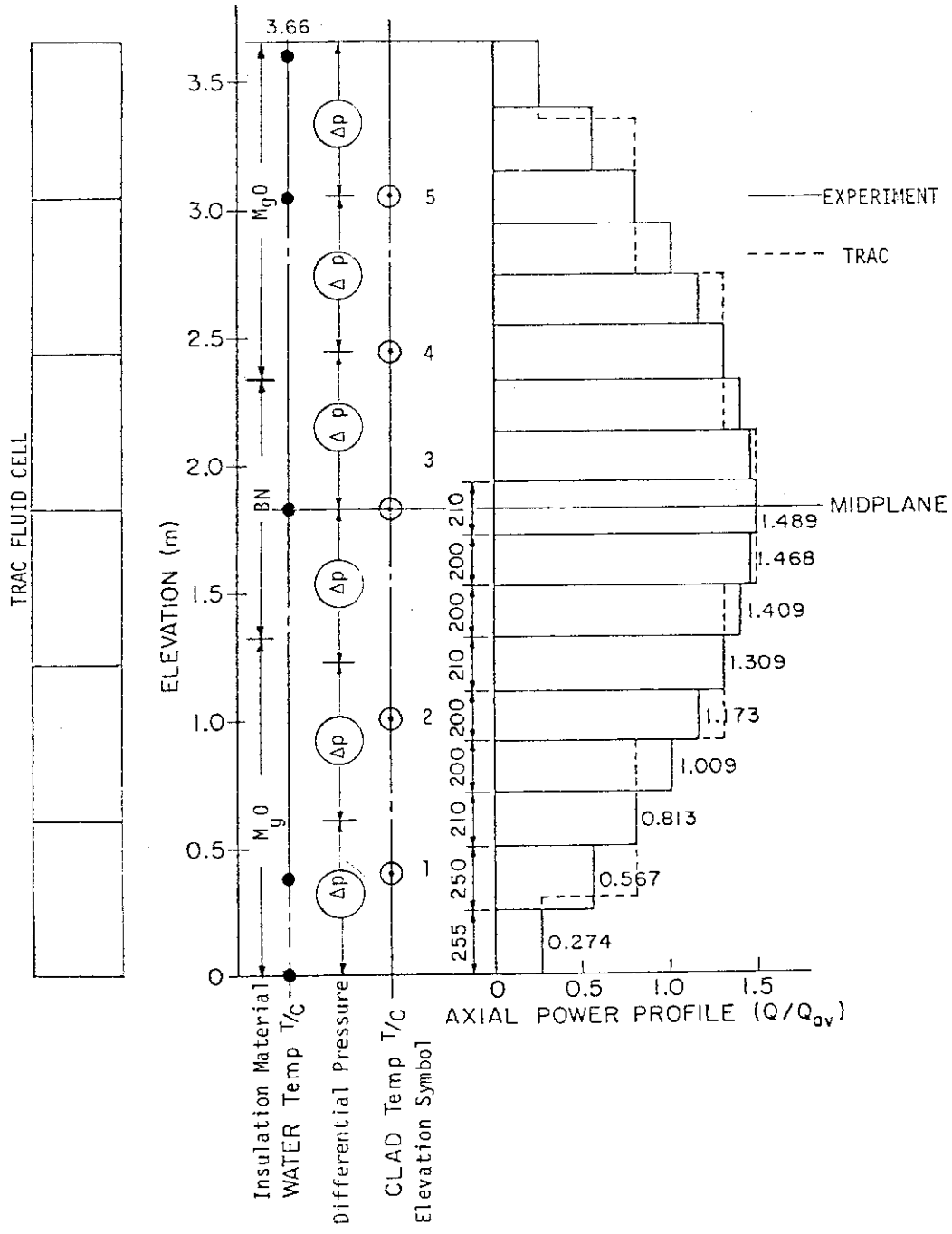

Fig. 3 Axial power profile, measurement locations, and TRAC noding in the core

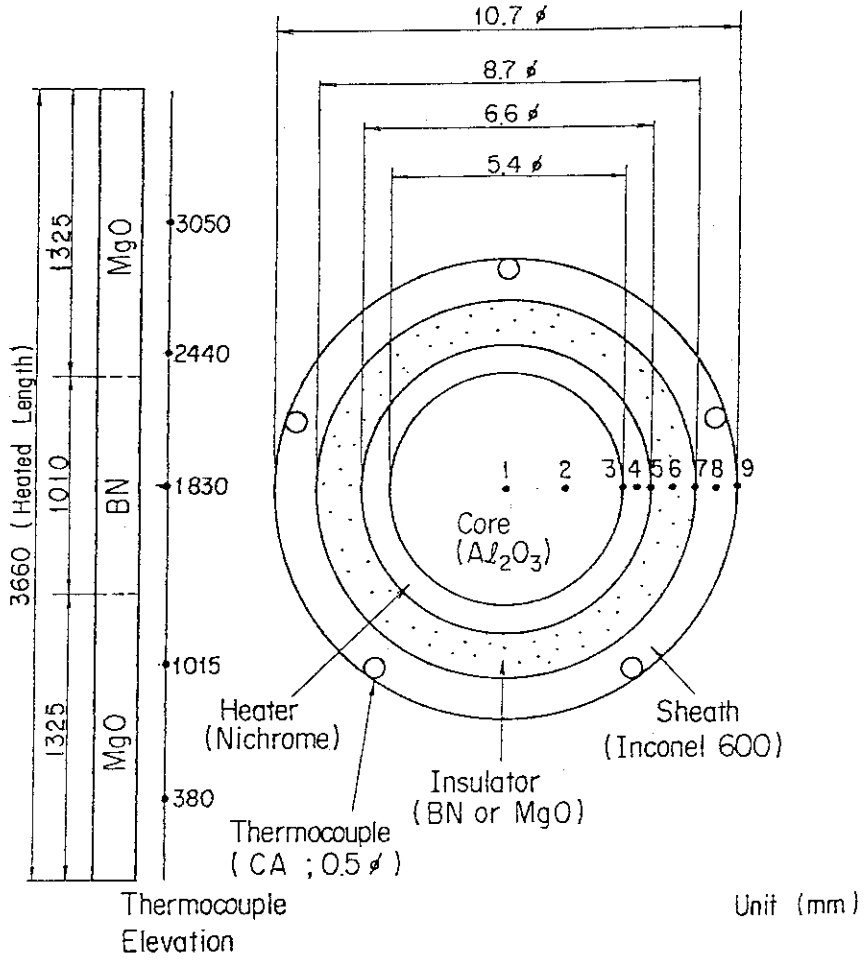

Fig. 4 Heater rod noding

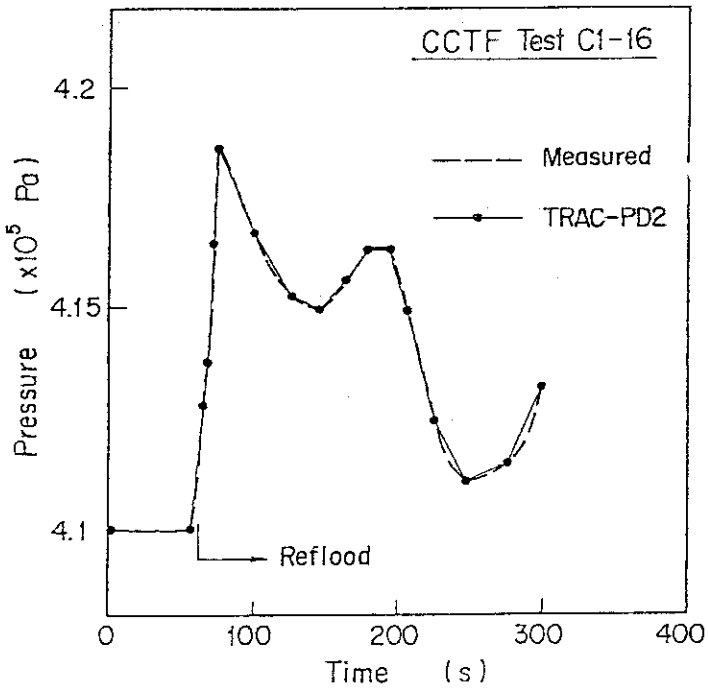

Fig. 5 Pressure in upper plenum

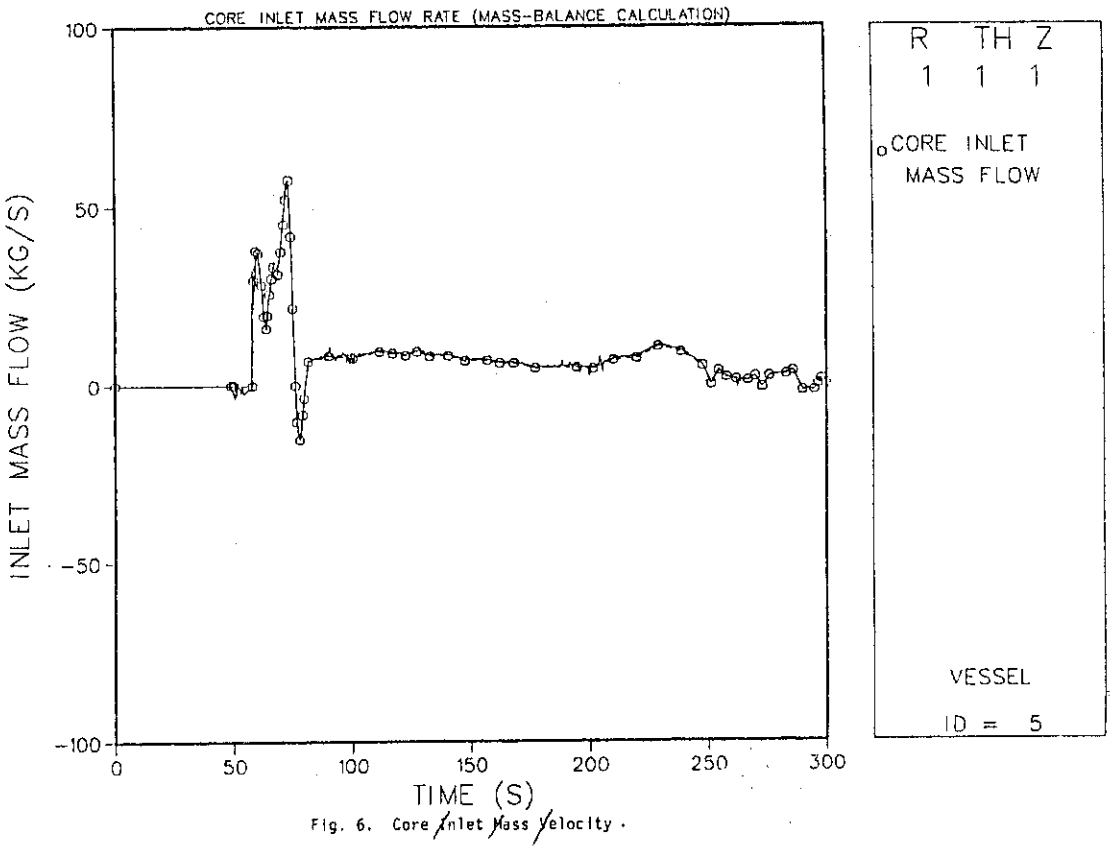

Fig. 6. Core inlet mass velocity.

Fig. 6 Core inlet mass flow rate

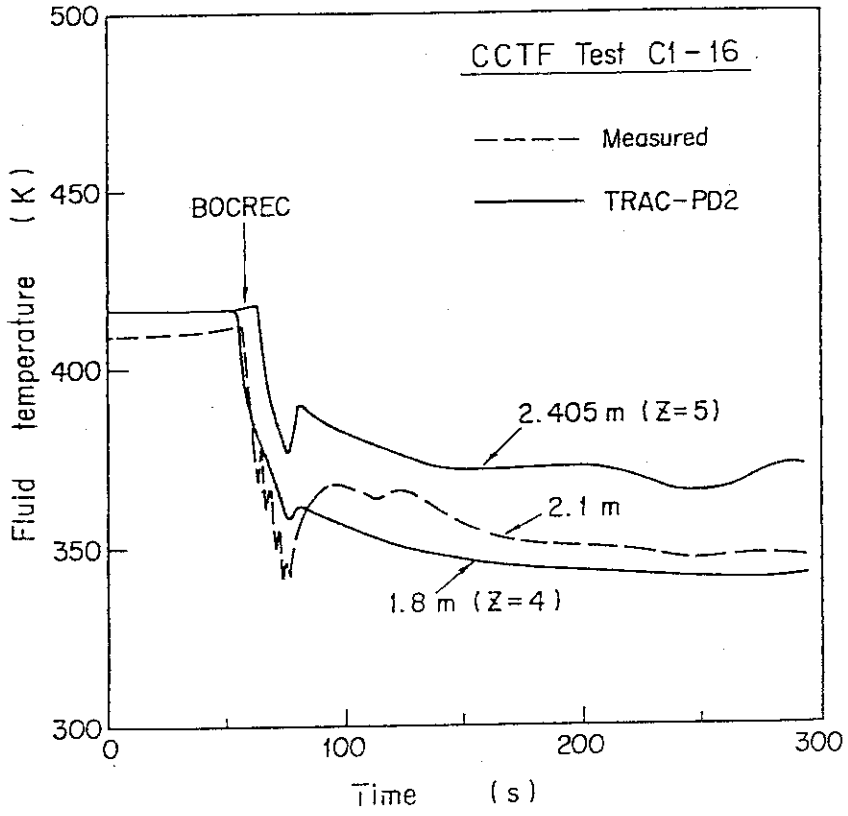

Fig. 7 Core inlet liquid temperature

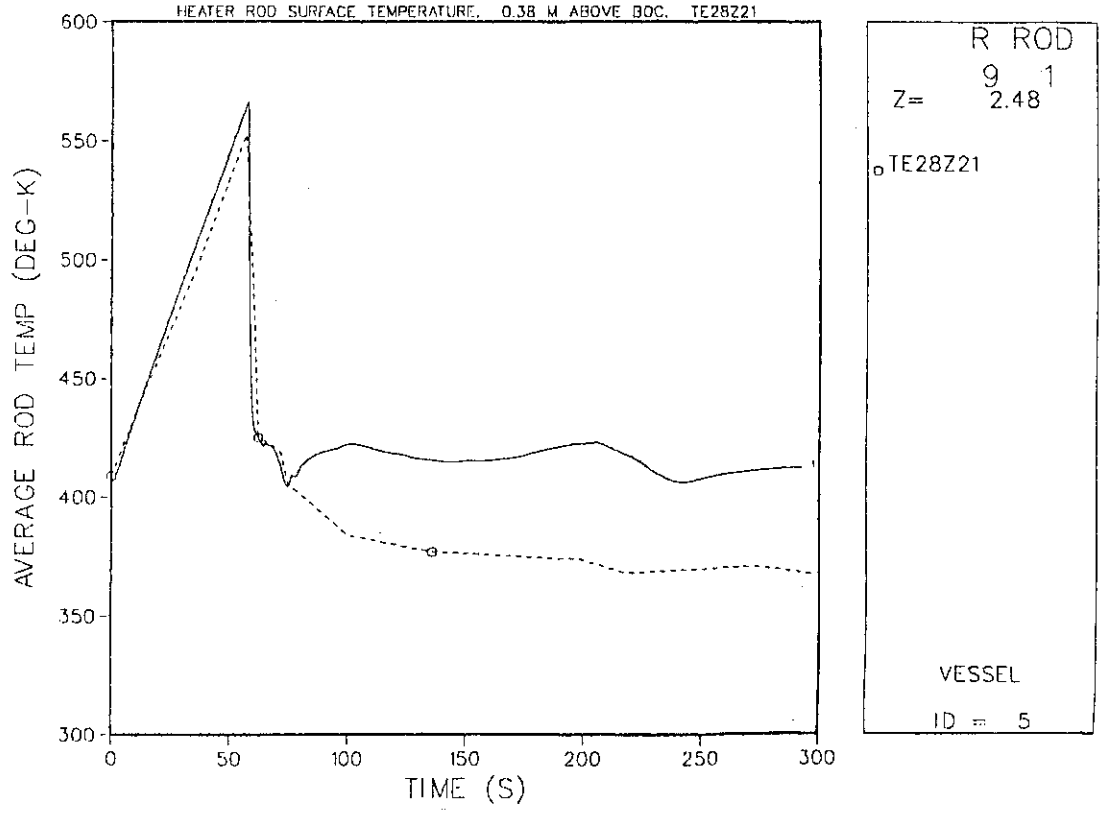

Fig. 8 Heater rod temperature at 0.38 m elevation

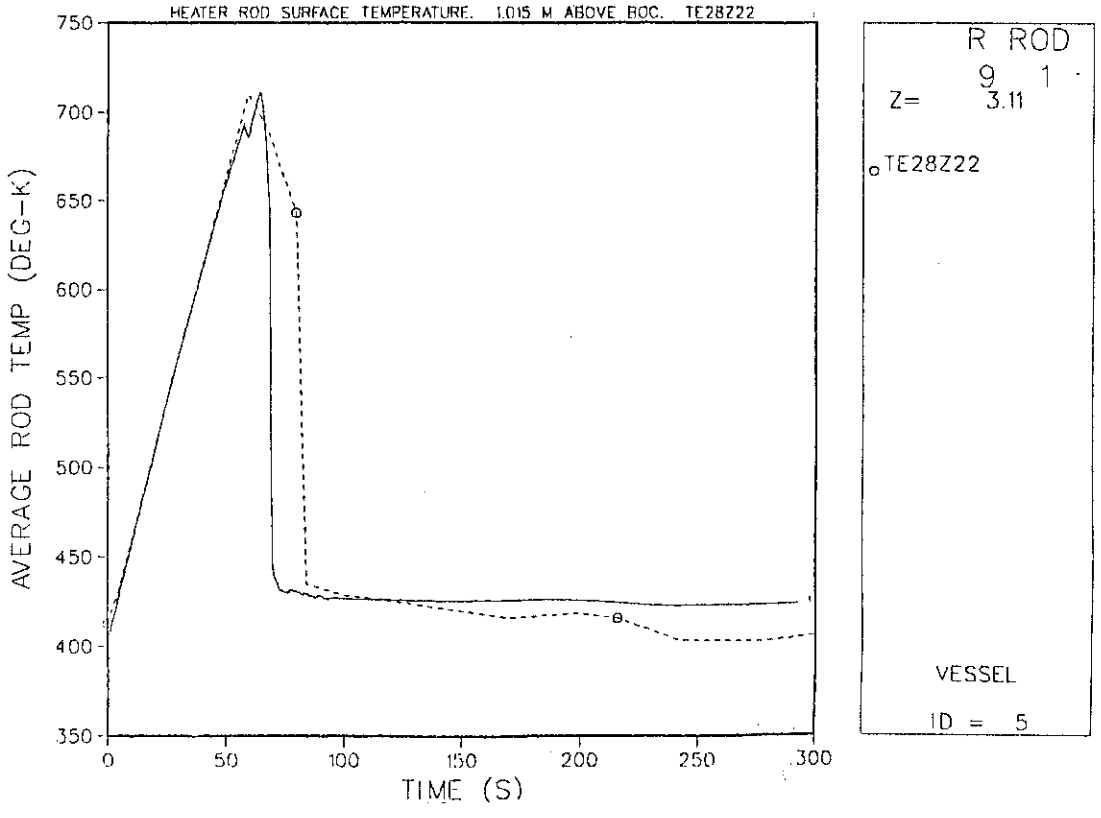

Fig. 9 Heater rod temperature at 1.015 m elevation

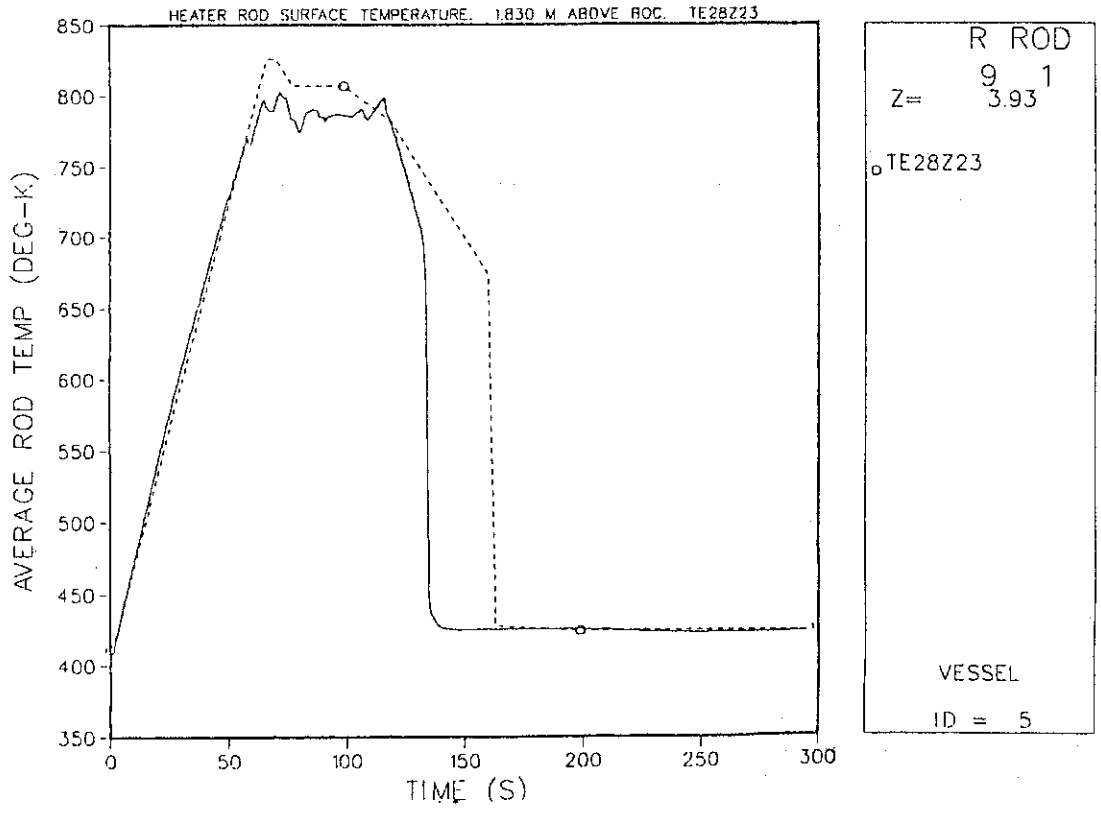

Fig. 10 Heater rod temperature at 1.83 m elevation

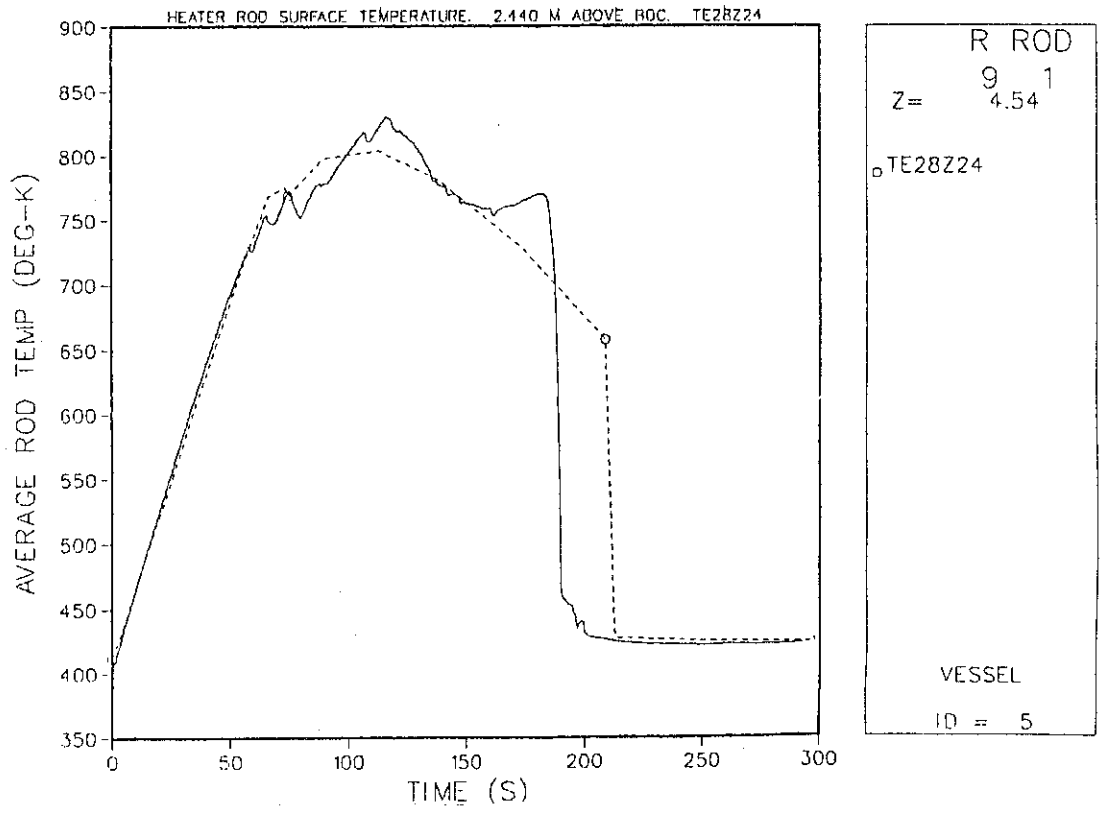

Fig. 11 Heater rod temperature at 2.44 m elevation

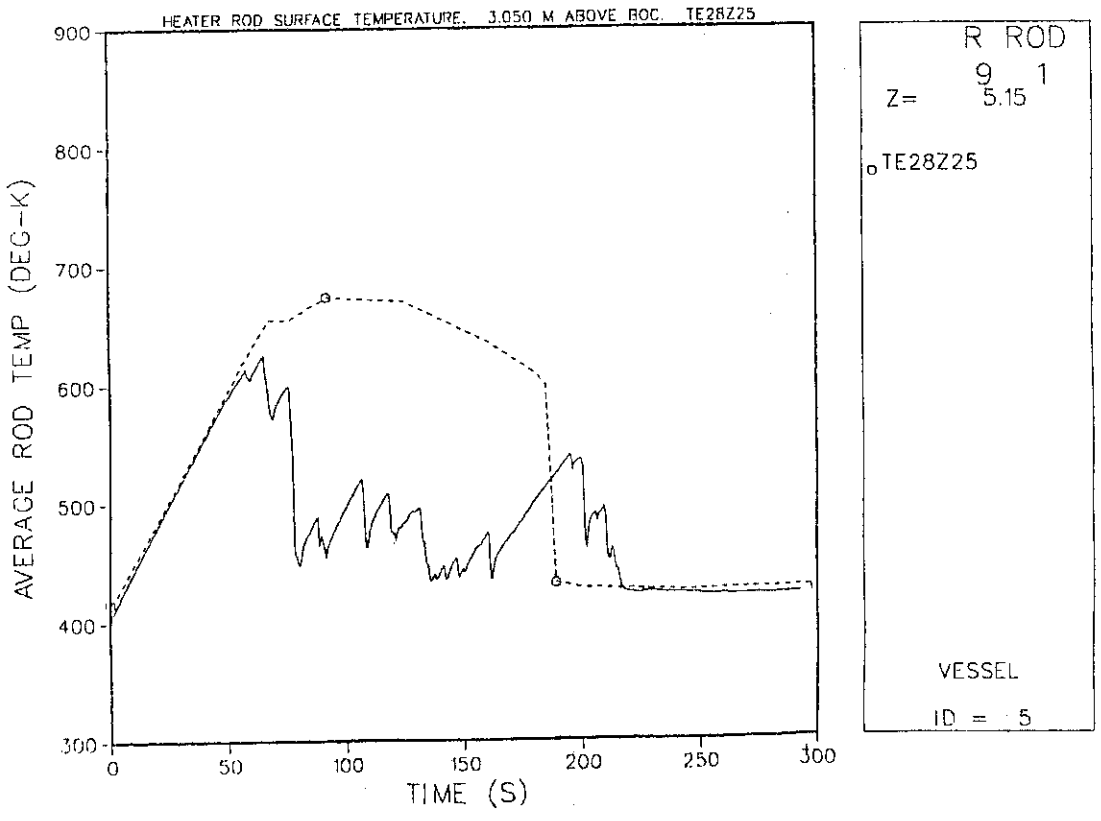

Fig. 12 Heater rod temperature at 3.05 m elevation

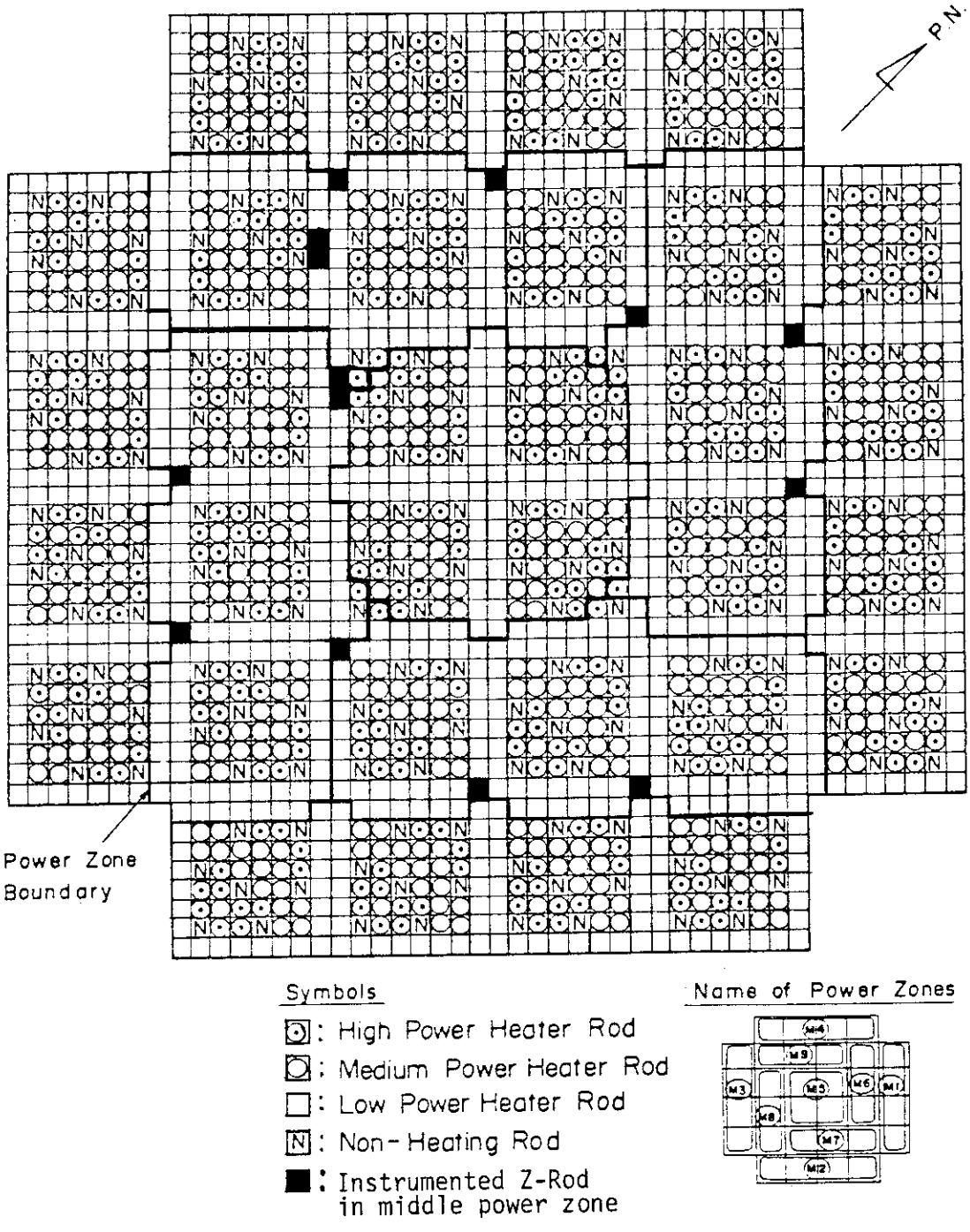

Fig. 13 Heater rod configuration of CCTF core

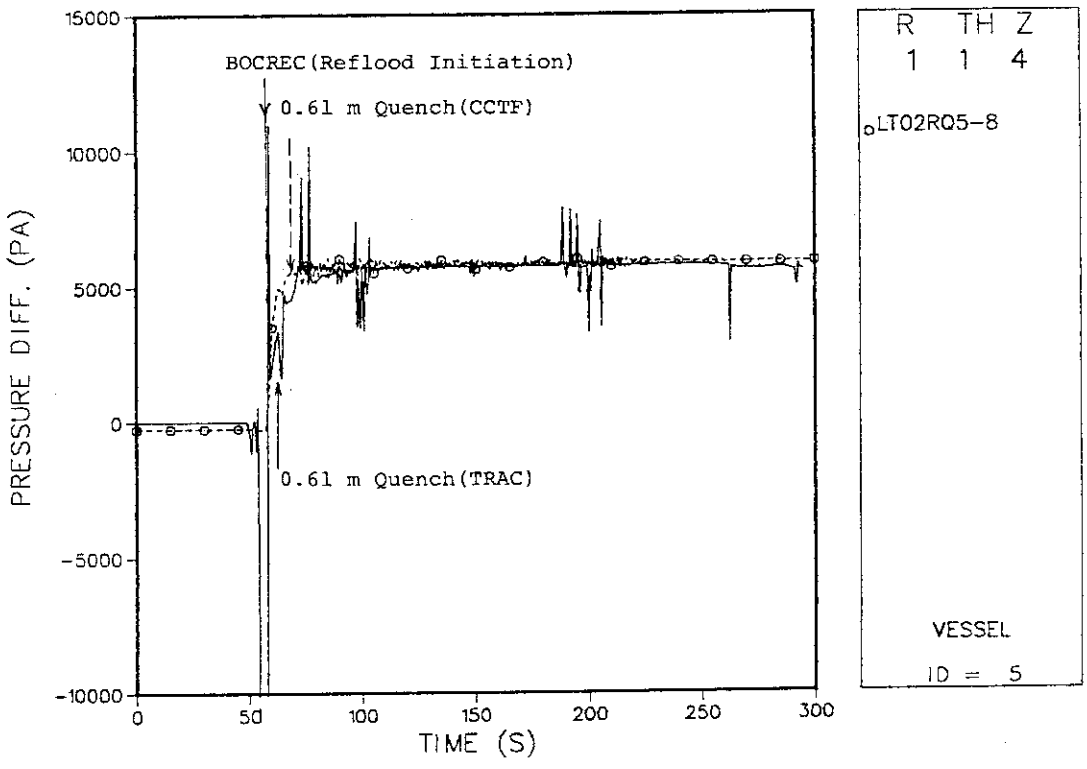

Fig. 14 Differential pressure in core 0-0.61 m

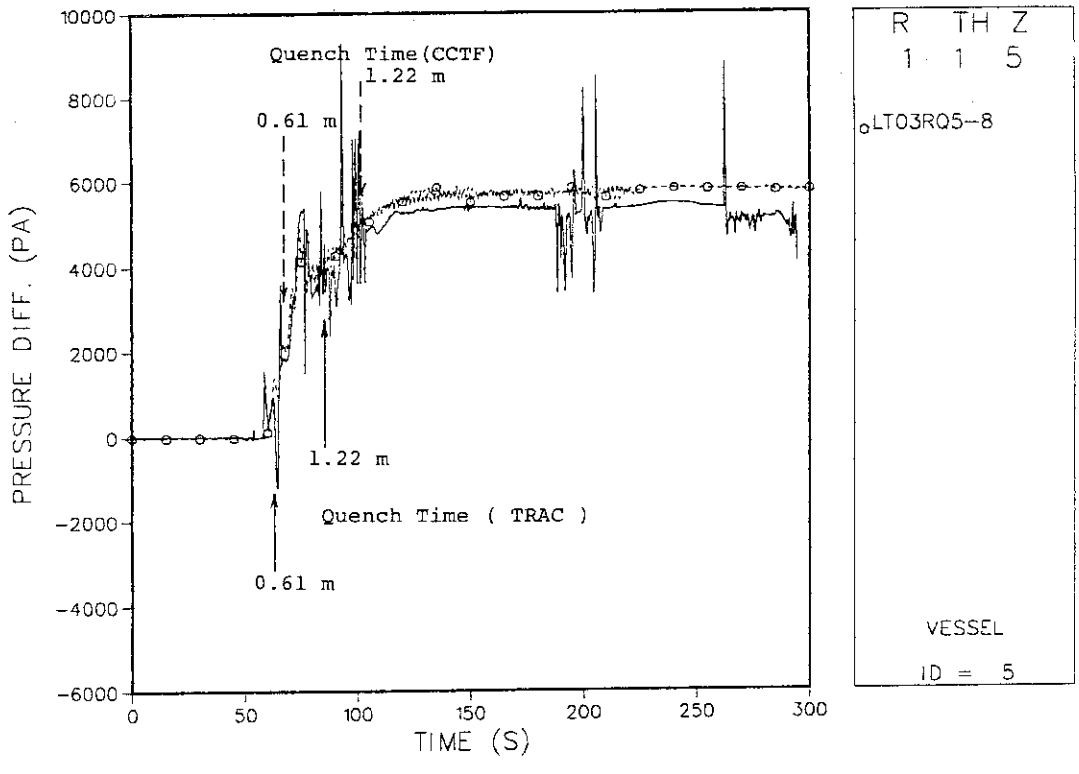

Fig. 15 Differential pressure in core 0.61-1.22 m

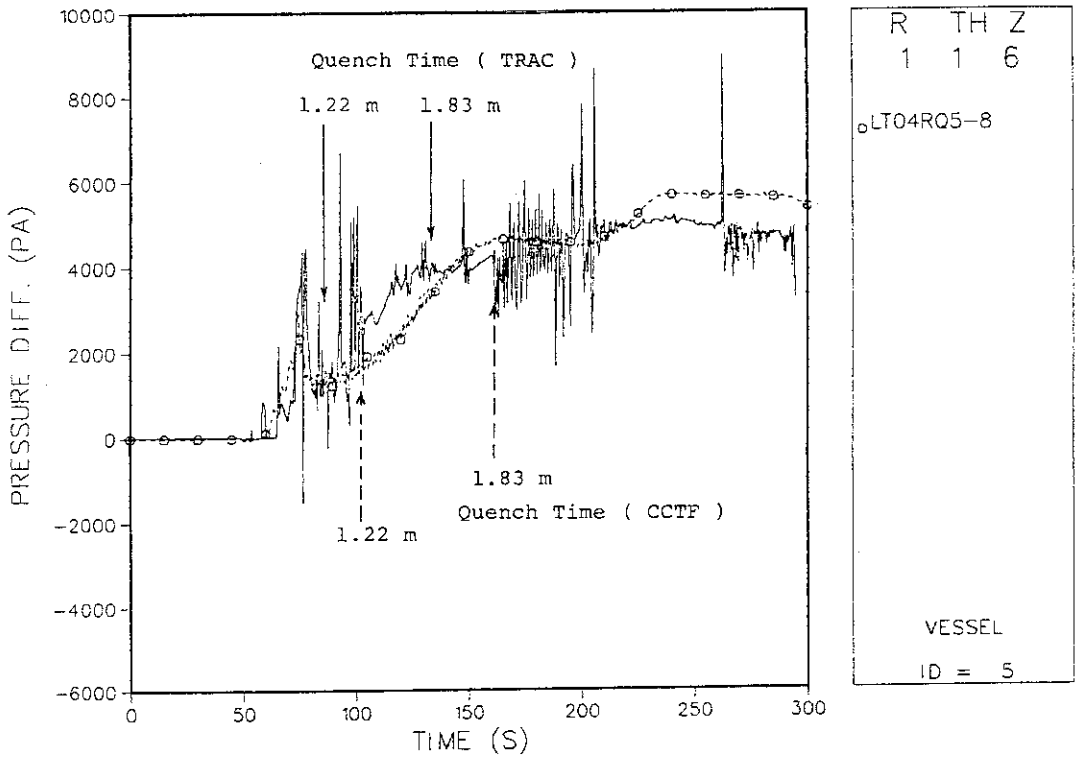

Fig. 16 Differential pressure in core 1.22-1.83 m

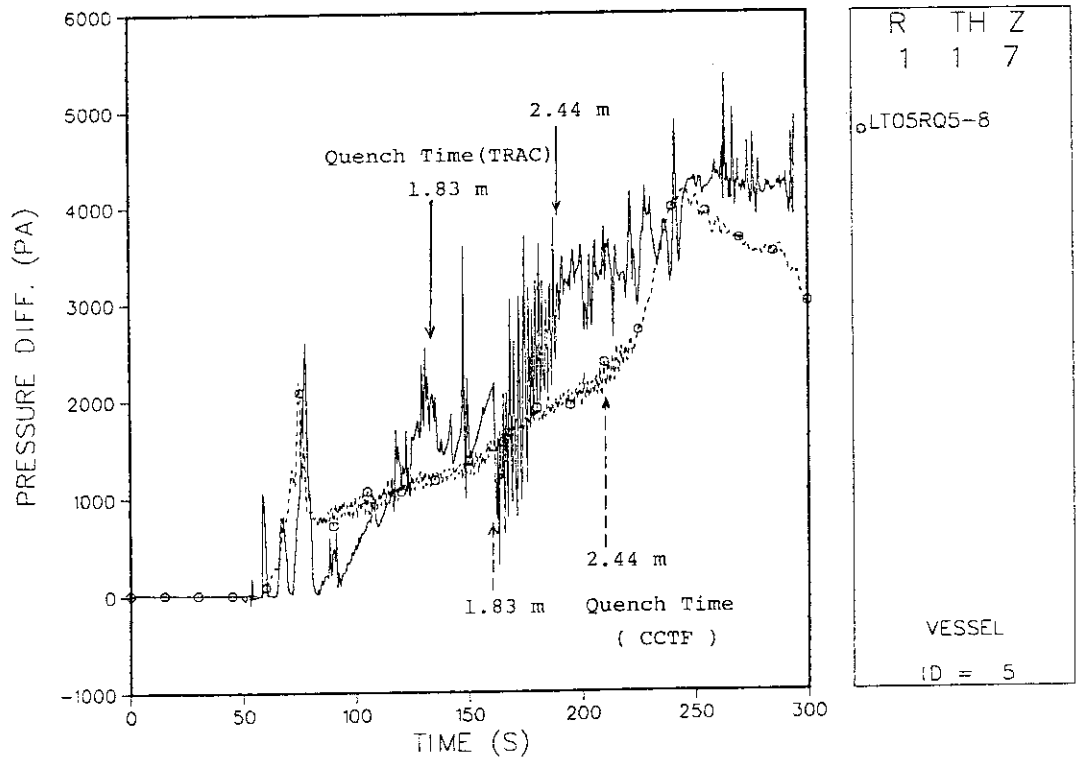

Fig. 17 Differential pressure in core 1.83-2.44 m

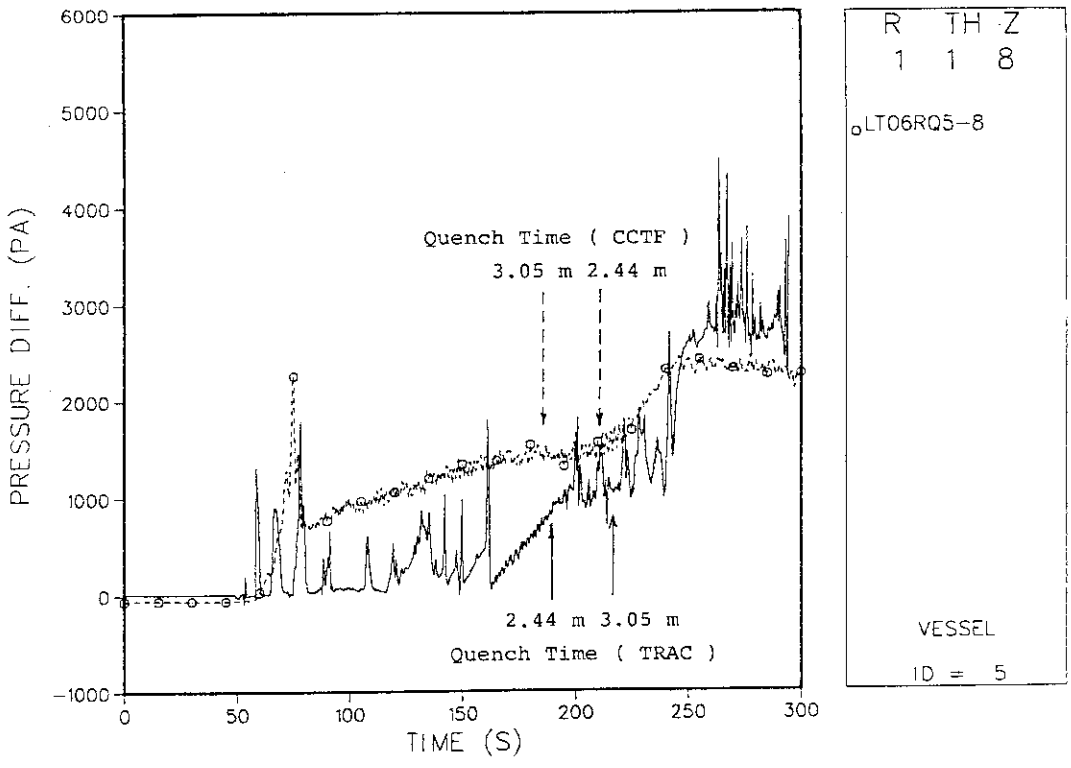

Fig. 18 Differential pressure in core 2.44-3.05 m

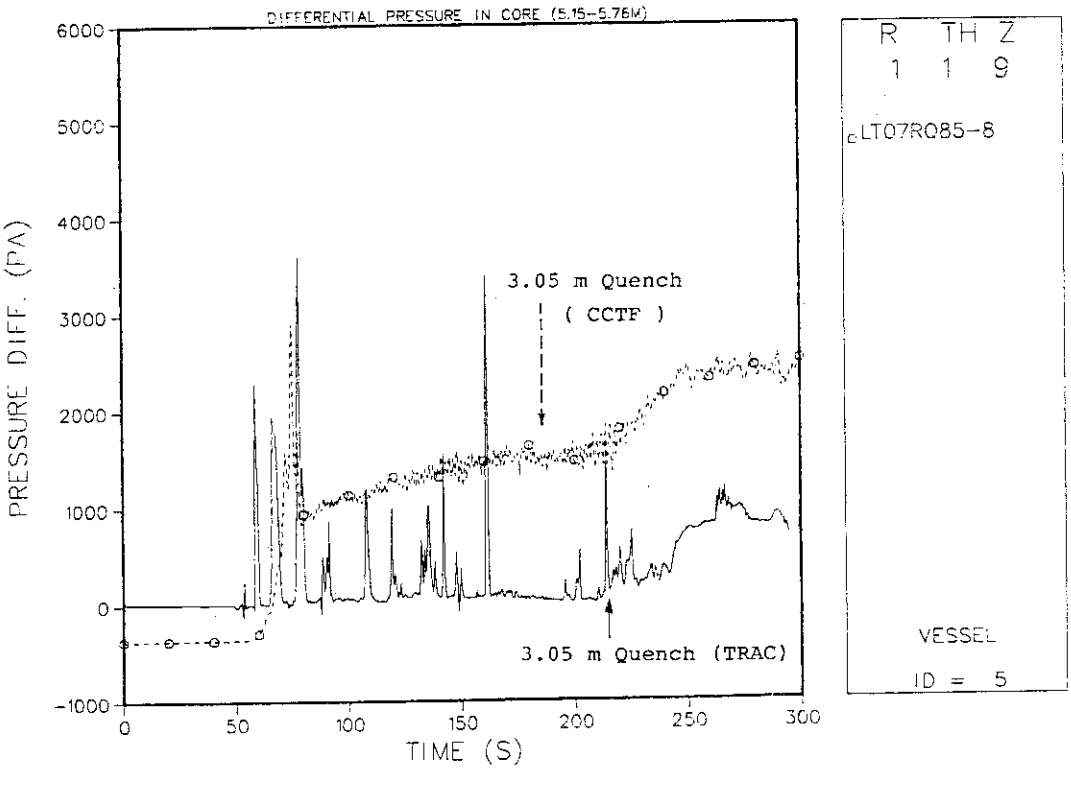

Fig. 19 Differential pressure in core 3.05-3.66 m

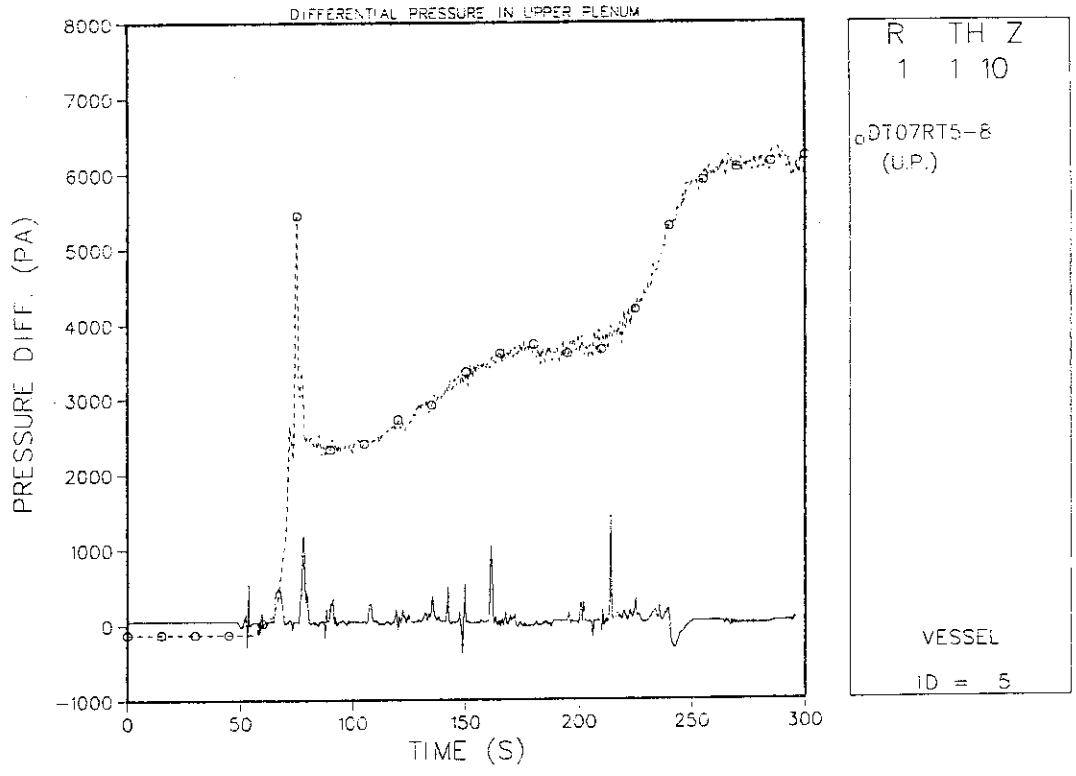

Fig. 20 Differential pressure in upper plenum

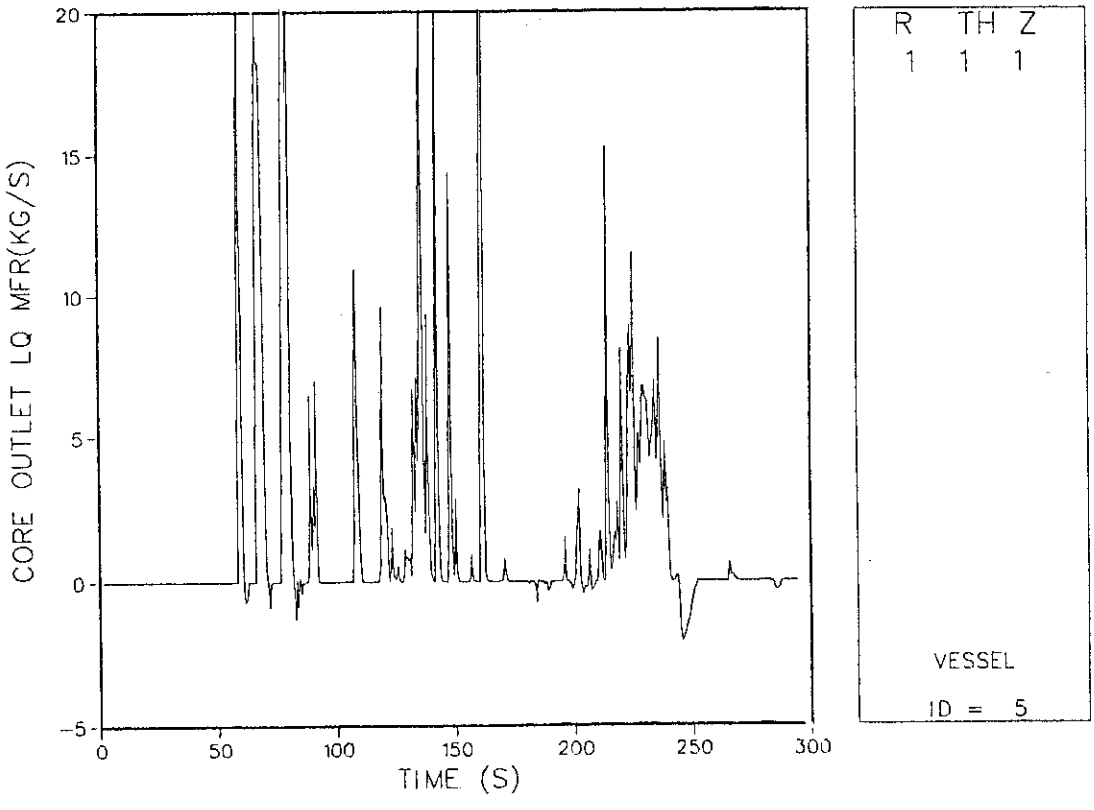

Fig. 21 Calculated core outlet liquid mass flow rate

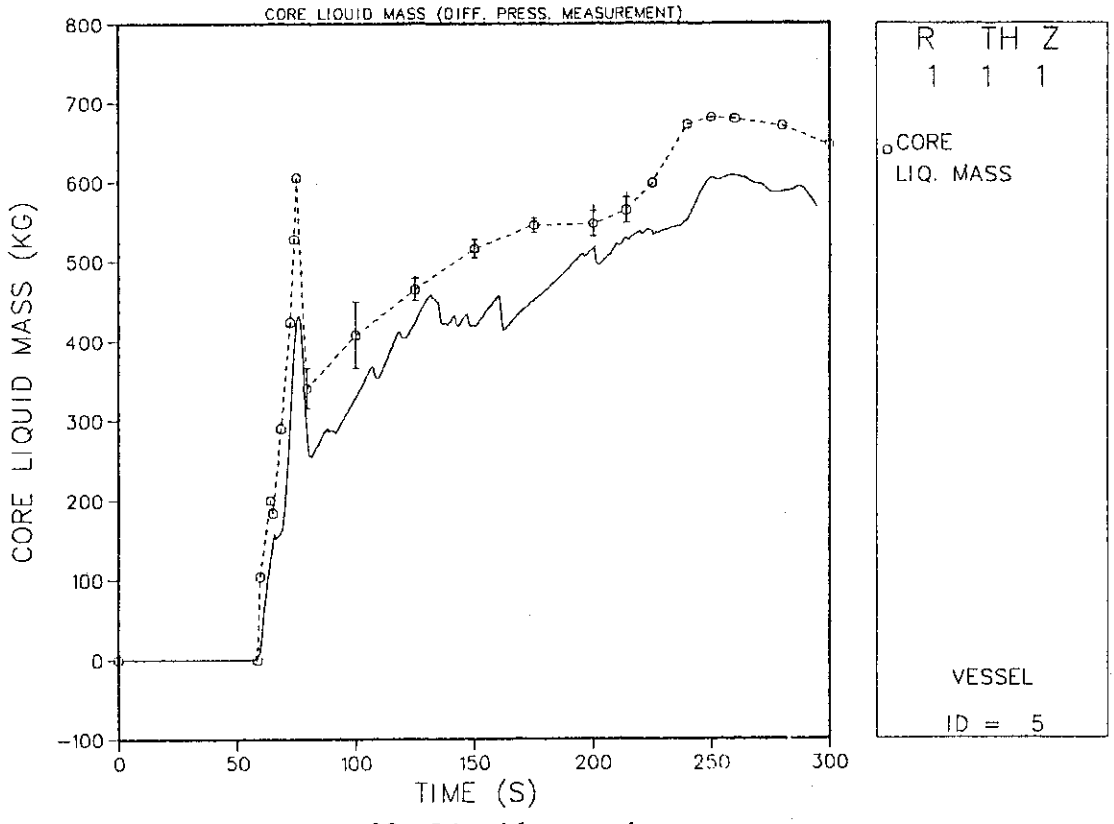

Fig. 22 Liquid mass in core

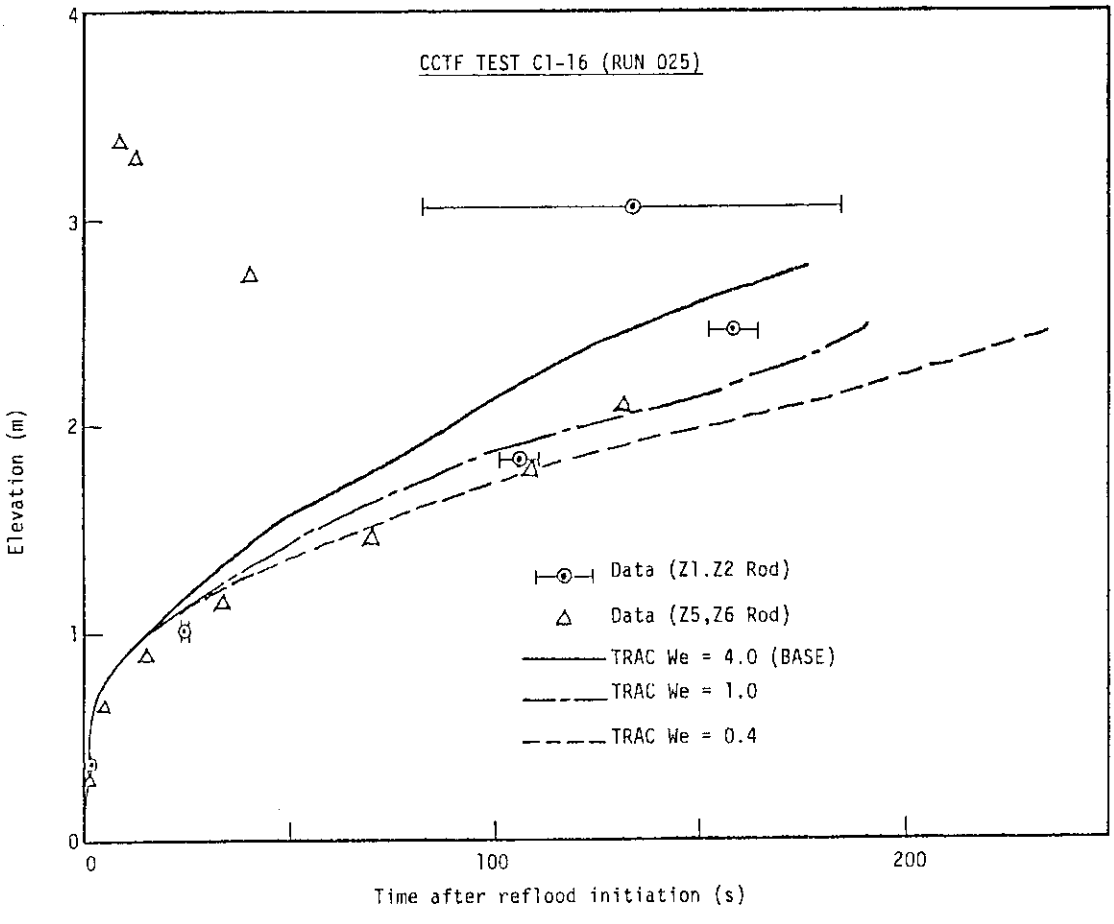

Fig. 23 Effect of critical Weber number on quench envelope

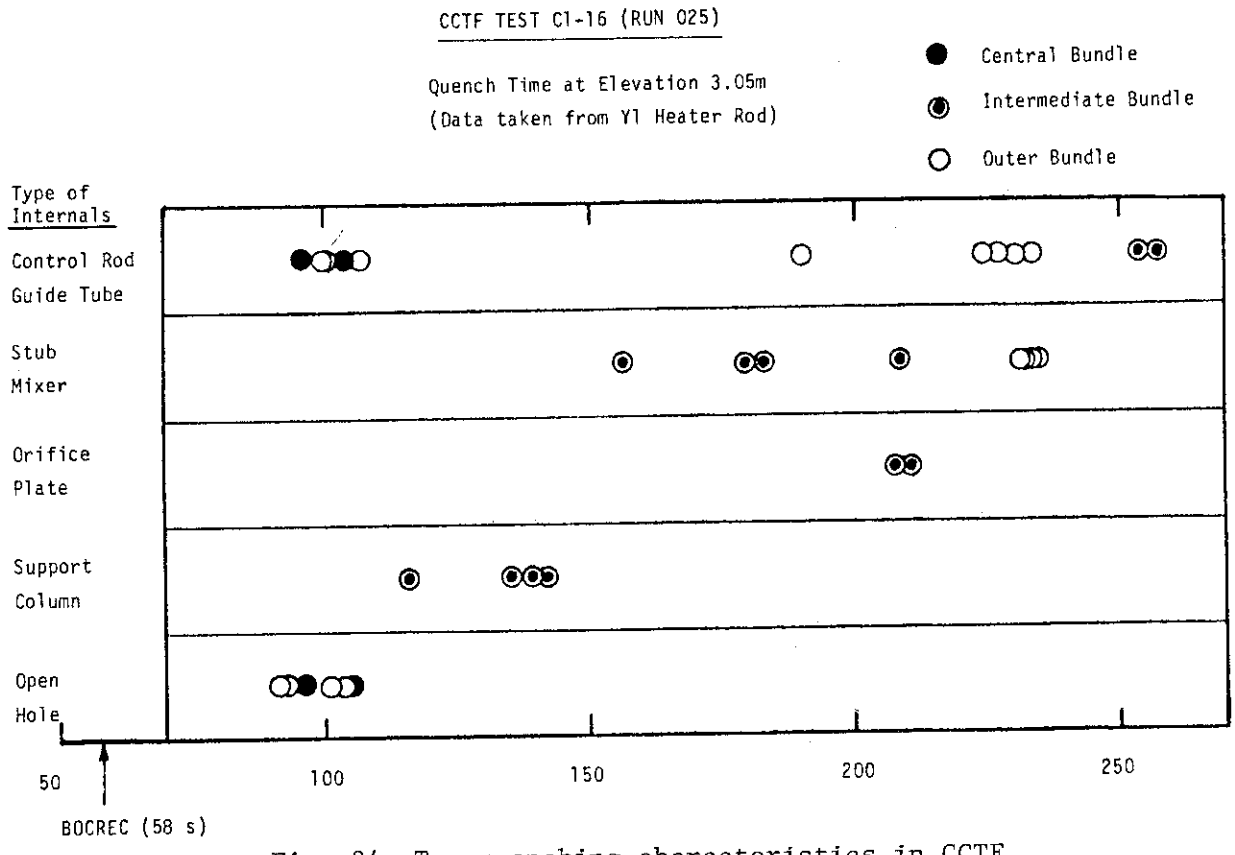

Fig. 24 Top quenching characteristics in CCTF

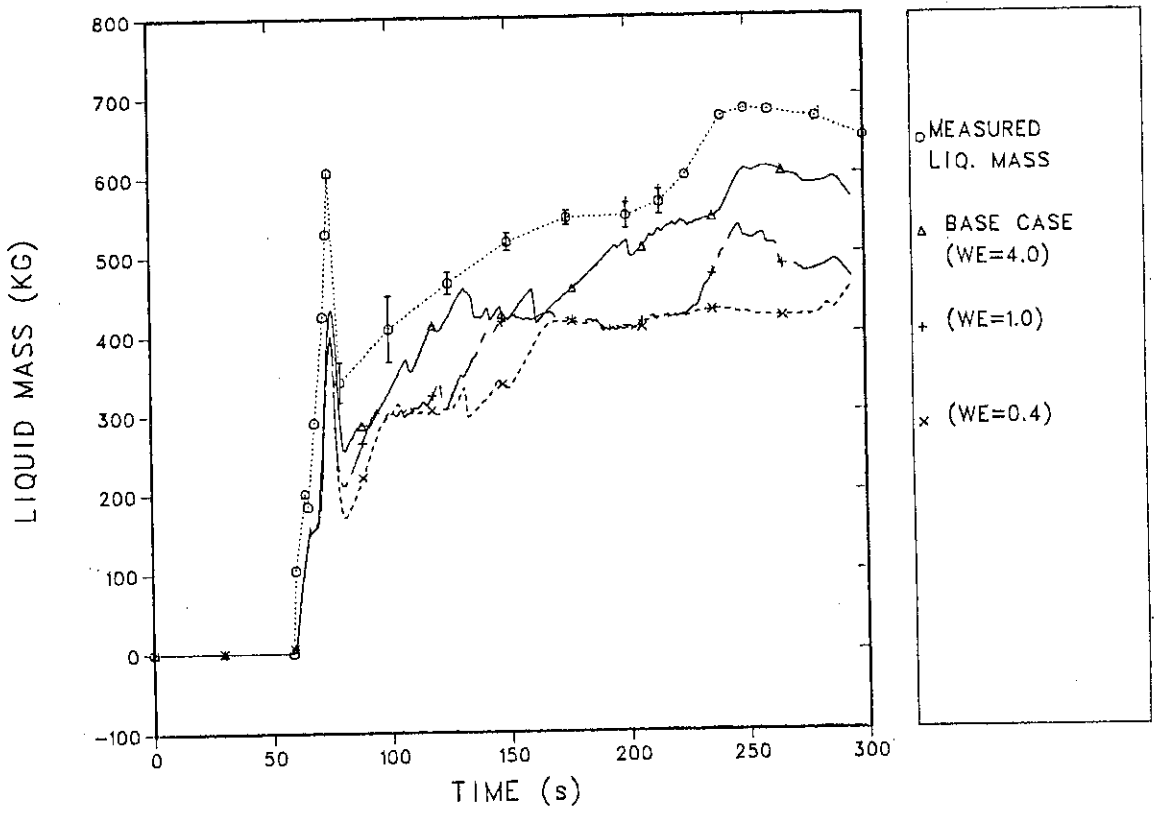

Fig. 25 Effect of critical Weber on liquid mass in core

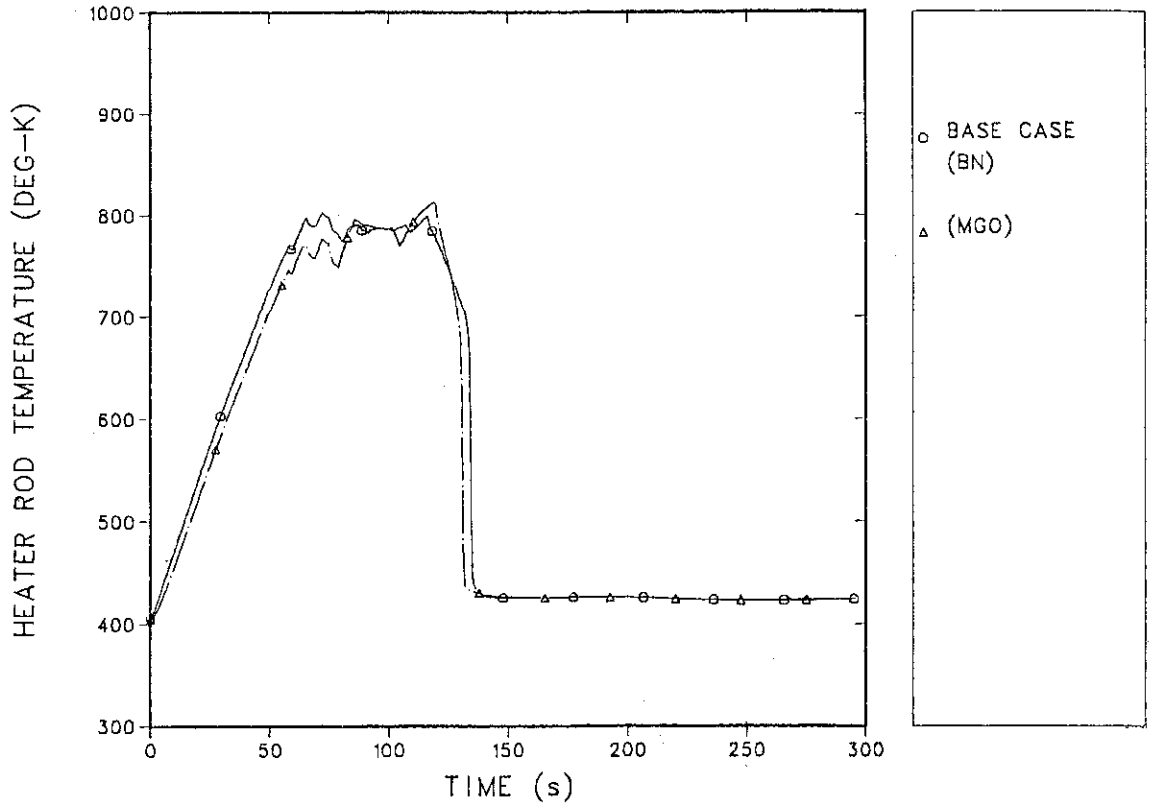

Fig. 26 Effect of material properties on heater rod temperature

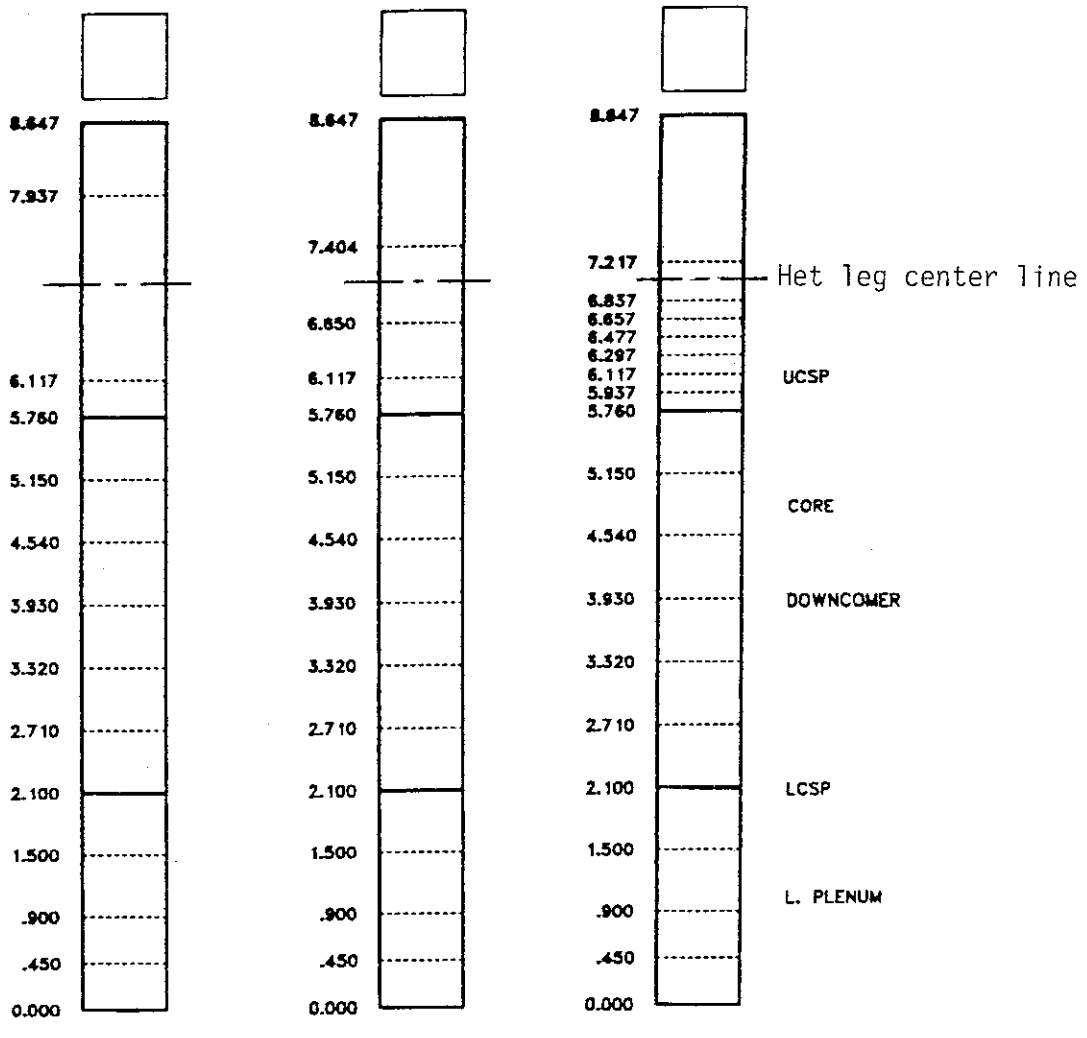

Fig. 27 Comparison of upper plenum noding

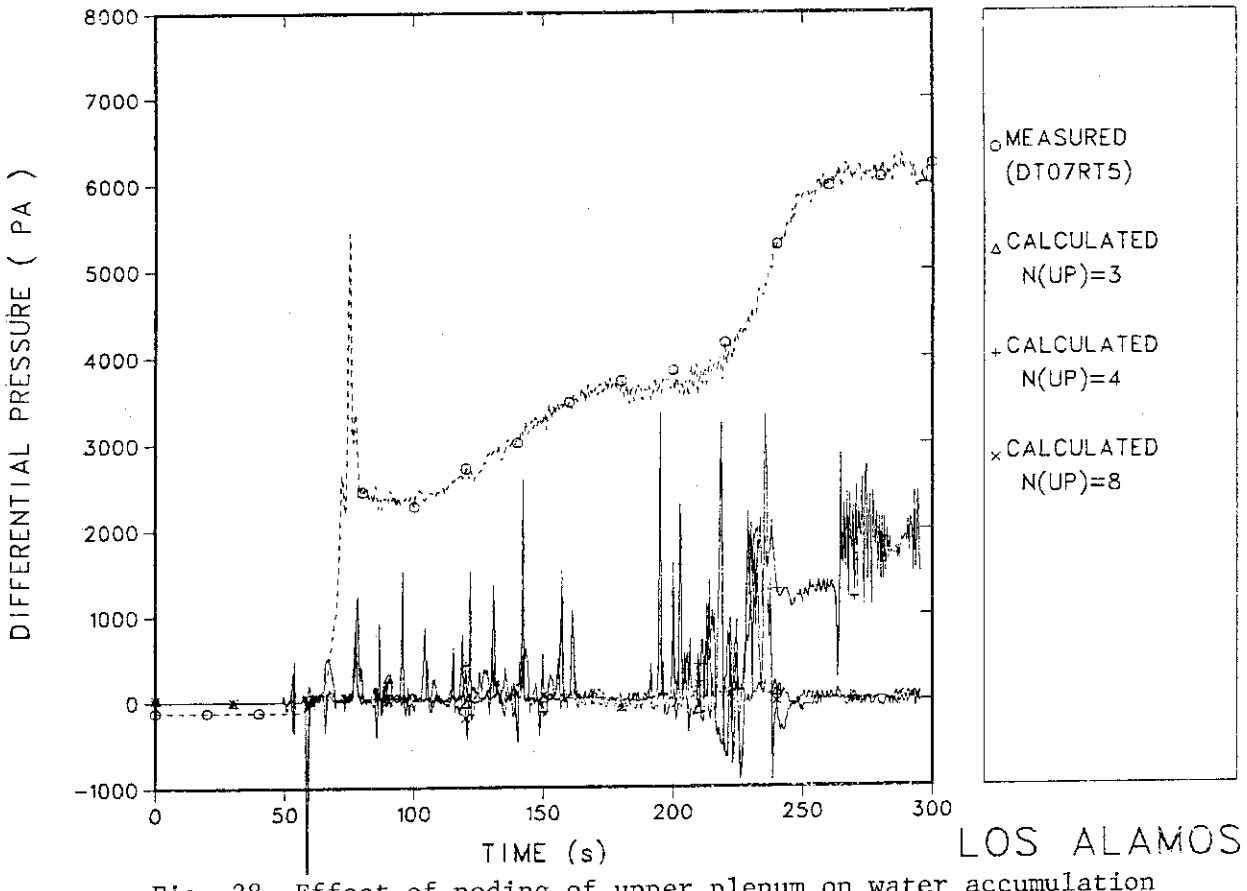

Fig. 28 Effect of noding of upper plenum on water accumulation

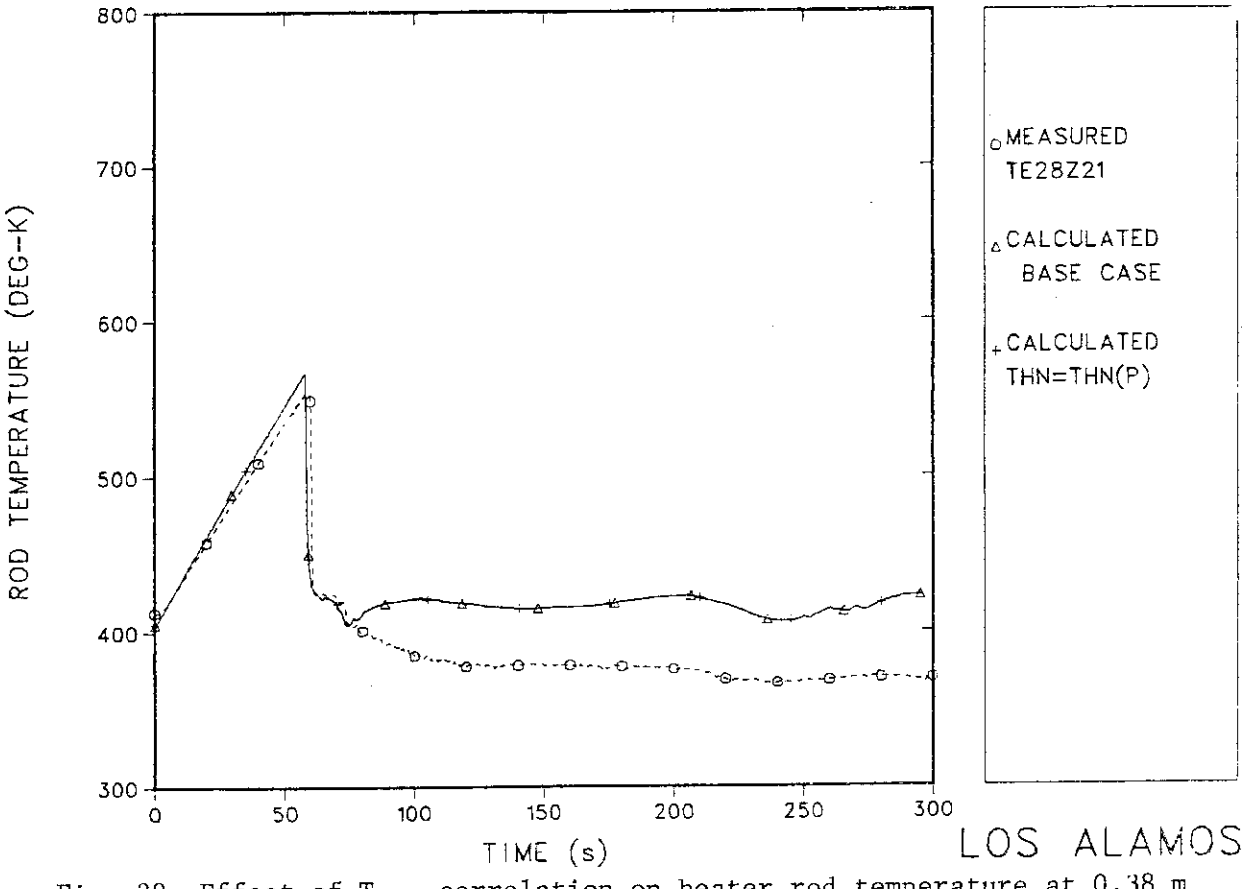

Fig. 29 Effect of T_{min} correlation on heater rod temperature at 0.38 m elevation

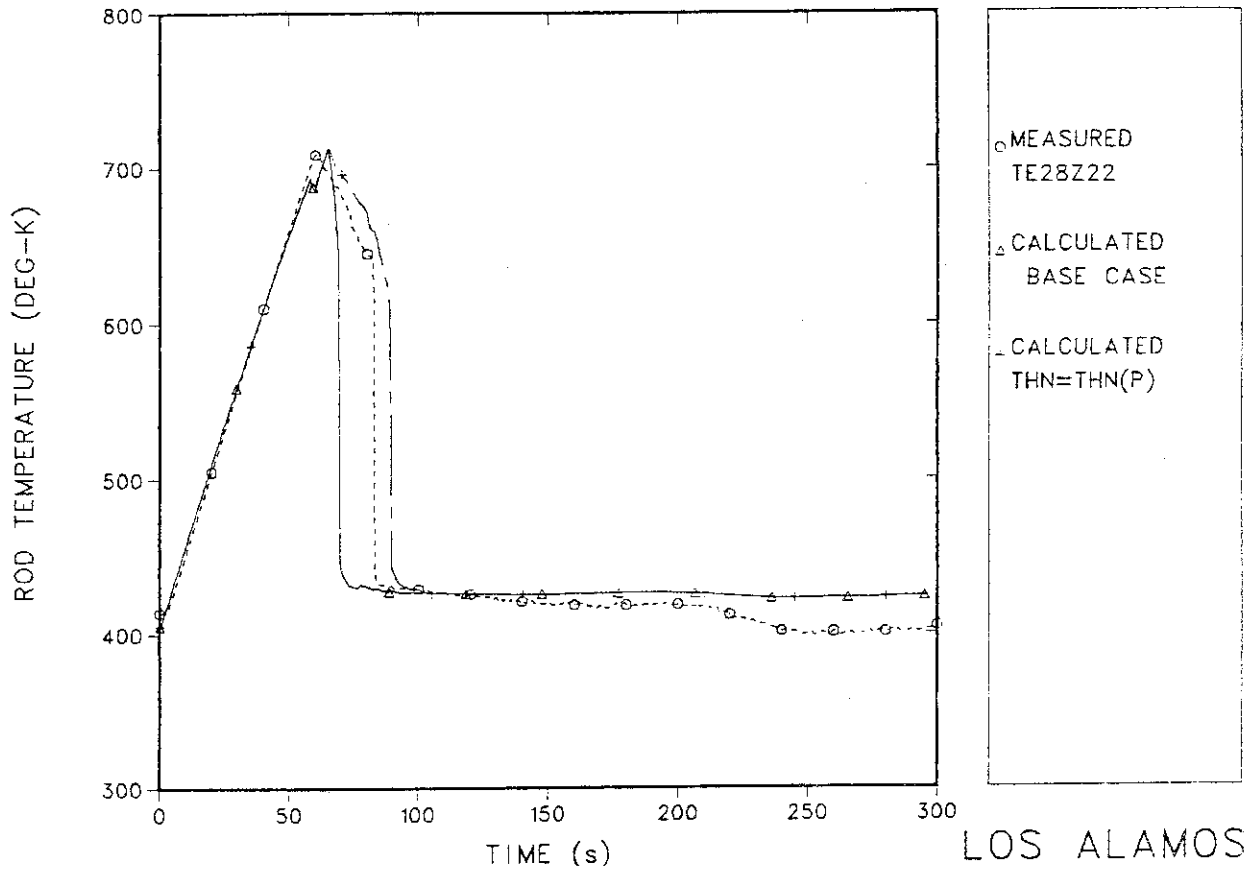

Fig. 30 Effect of T_{min} correlation on heater rod temperature at 1.015 m elevation

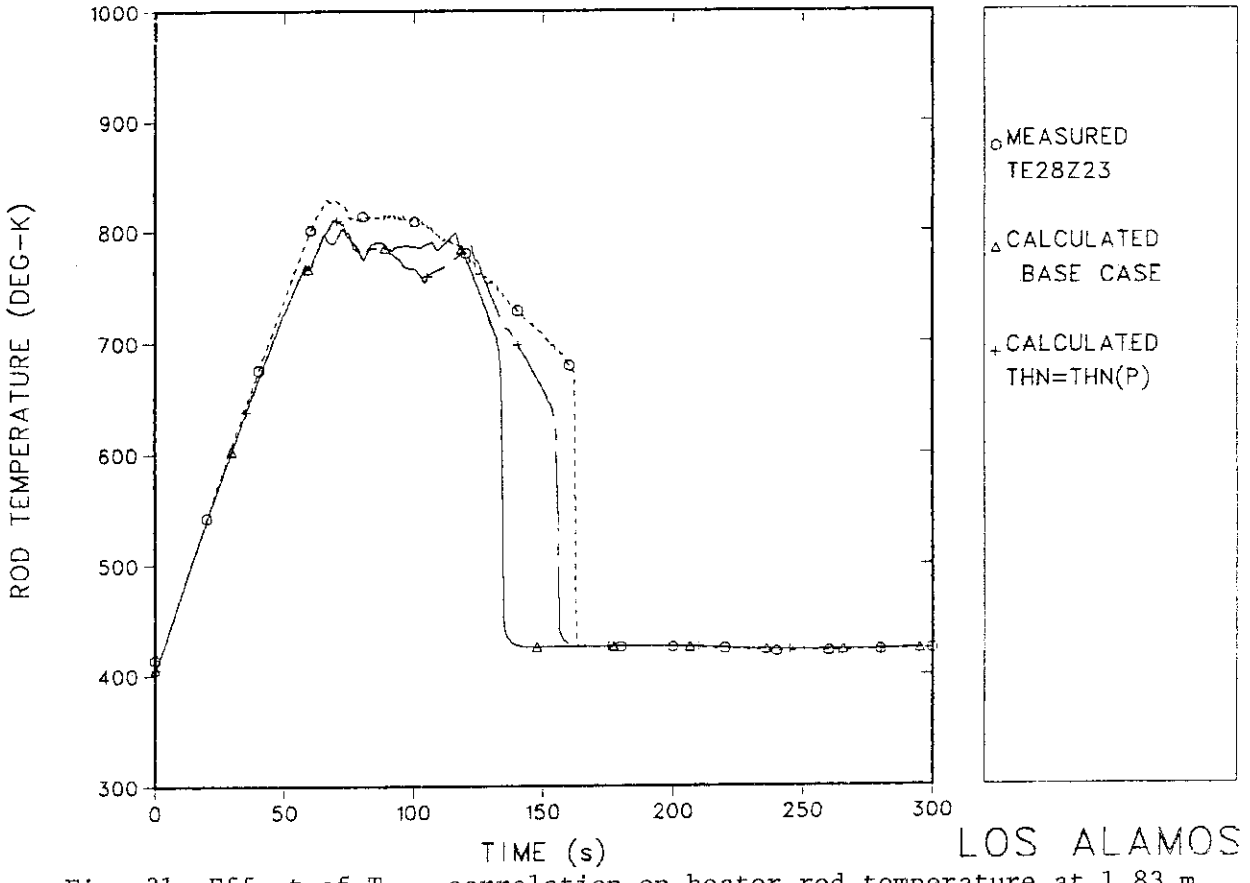

Fig. 31 Effect of T_{min} correlation on heater rod temperature at 1.83 m elevation

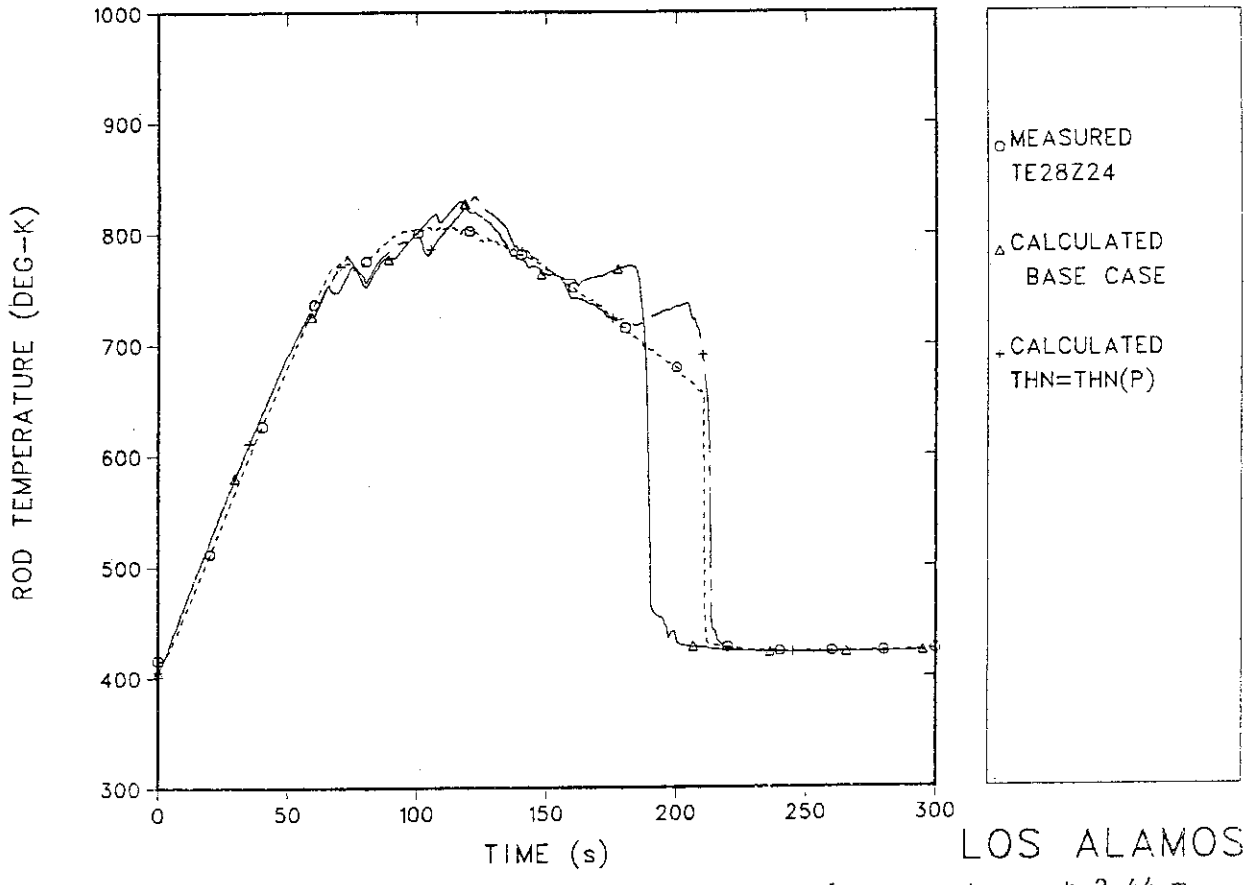

Fig. 32 Effect of T_{min} correlation on heater rod temperature at 2.44 m elevation

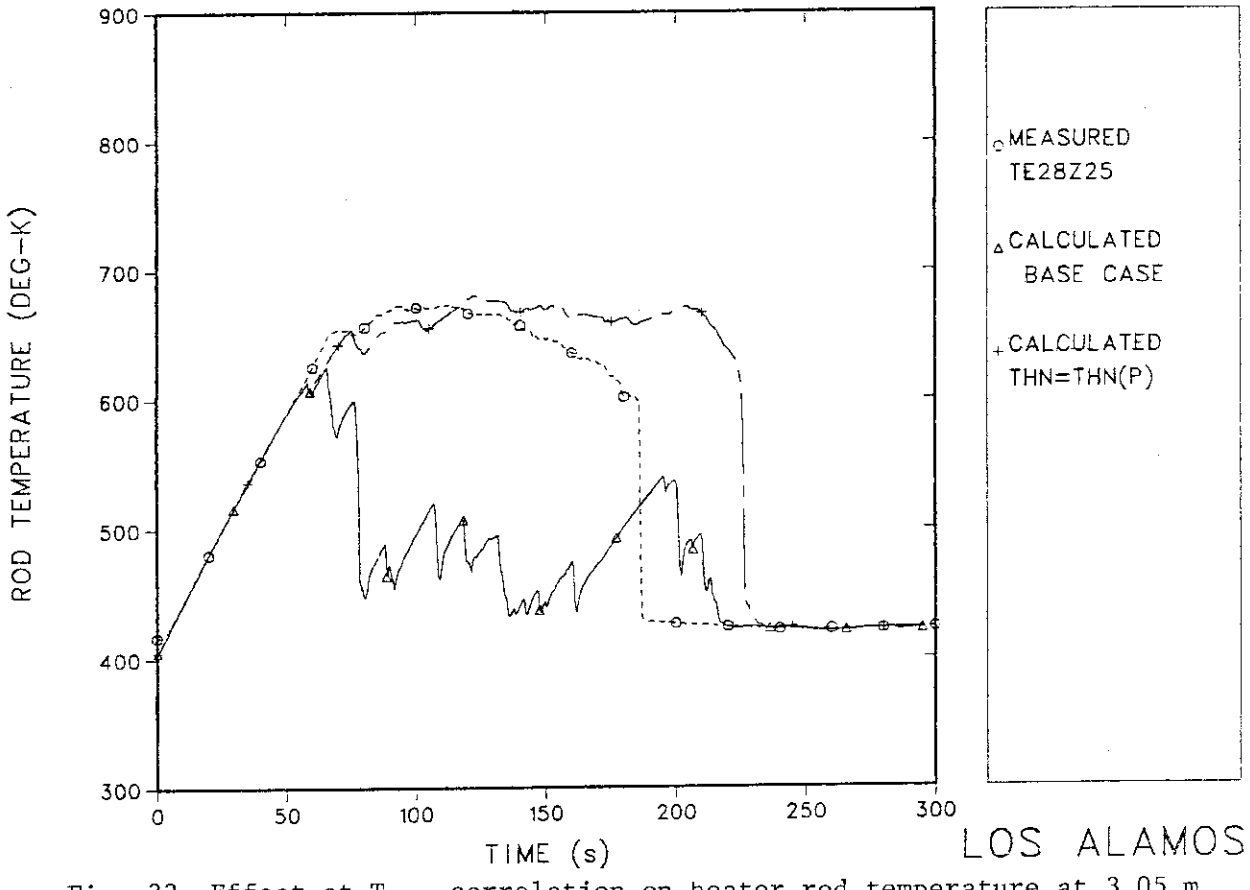

Fig. 33 Effect of T_{min} correlation on heater rod temperature at 3.05 m elevation

APPENDIX

```
            4
 CYLINDRICAL CORE TEST FACILITY
  POST TEST ANALYSIS - TEST C1-16(RUN 025)
    FLECHT COUPLING TEST - RUN 31058
     SINGLE TUBE MODEL    * BASE CASE CALCULATION *
             0  0.                    1
             0                1       5              4              1
   .100000E-02    .100000E-04    .100000E-02  0.
            10                0      10              3              1
 0           1  0             2  0           3  0           4  0           5E
             2
             1                0          49.0  0.
             1                6             1           0
             2                0          49.0         9.0
             1                6             1           0
             3                0          49.0      1000.0
             1                6             1           0
FILL                          1             1           .                    CARD 1
             1                4             1          61                    CARD 2
     4.500E-01     8.513E-03           0.0          0.0          340.0      CARD 3
     4.100E+05                                                               CARD 4
           0.0            0.0           1.0         3.70S                    VMTB
           9.0           3.70          9.54         1.71S
         10.39           2.17         11.53         2.13S
         12.85           1.63         13.82         1.12S
         14.95          0.932         15.45         1.14S
         16.23           1.48         17.13         1.73S
         17.92           1.92         19.84         1.80S
         21.05           2.15         22.25         2.59S
         23.06           3.00         24.30         3.30S
         25.27           2.40         26.00         1.25S
         27.10           0.00         27.60        -0.595S
         28.90         -0.884         30.10        -0.476S
         30.70         -0.209         32.50         0.392S
         41.20          0.489         51.20         0.449S
         62.60          0.546         68.00         0.519S
         73.50          0.482         78.40         0.546S
         83.70          0.472         91.50         0.481S
         98.60          0.392        108.0          0.402S
         113.2          0.359        119.2          0.357S
         128.2          0.274        145.7          0.283S
         152.6          0.263        161.2          0.402S
         171.0          0.437        180.0          0.617S
         189.7          0.530        198.8          0.305S
         202.5          0.000        205.5          0.222S
         209.0          0.115        213.0          0.076S
         218.0          0.061        221.0          0.131S
         224.0         -0.049        227.0          0.131S
         234.0          0.162        237.0          0.213S
         241.0         -0.101        246.0         -0.097S
```

```
          247.5          0.0          249.0          0.081S
          251.0            0.0E
VALVE                         2              2
              3               0              2              1              6
              0               0
      1.552E-01      5.000E-03            0.0            0.0            0.0
            0.0
              4               1              2              0              2
      1.892E-02      1.552E-01              0
F     4.500E-01E
F     8.513E-03E
F     1.892E-02E
F           0.0E
F           0.0E
F     1.552E-01E
F            1E
F           0.0E
F           0.0E
F         340.0E
F         400.2E
F     4.100E+05E
            0.0            0.0            0.5           1.0E                          VLTB
PIPE                          3              3                                        OUTLET
              1               0              3              4              6  CARD 2
              0               0                                                CARD 3
      3.104E-01      5.000E-03            0.0            0.0            0.0  CARD 4
            0.0
F     4.645E-01E
F     3.515E-02E
F     7.567E-02E
F           0.0E
F           0.0E
F     1.552E-01E
F            1E
F           1.0E
F           0.0E
F         405.0E
F         405.0E
F     4.100E+05E
BREAK                         4              4                                        CARD 1
              4               1             28              3                  CARD 2
      1.552E-01      8.787E-03            1.0          405.0      4.100E+05  CARD 3
            0.0       4.10E+05           57.0      4.10E+05S                  PTB
           64.4       4.30E+05           67.7      4.42E+05S
           72.7       4.69E+05           75.1      4.90E+05S
          100.0       4.72E+05          127.4      4.58E+05S
          146.8       4.54E+05          164.3      4.60E+05S
          181.0       4.66E+05          194.4      4.66E+05S
          207.9       4.56E+05          226.6      4.33E+05S
          248.1       4.20E+05          276.2      4.24E+05S
          300.0       4.40E+05          314.1      4.69E+05S
          325.2       5.03E+05          348.7      4.95E+05S
          372.1       4.50E+05          392.2      4.24E+05S
          400.0       4.20E+05          439.0      4.23E+05S
          457.3       4.31E+05          469.3      4.48E+05S
          486.1       4.20E+05          500.0      4.13E+05E
VESSEL                        5              5
             13               1              1              2
              0               0              0             10              4
```

```
                1
                0              0              0              1
             10.0           75.0       5.0E-03
           8026.0          502.0           17.3            0.6        60000.0
          1.33645
                9             10              7              2
                1              0              0              0            120
       9.82000E6
            0.45S
            0.90           1.50            2.1           2.71           3.32
            3.93           4.54           5.15           5.76          6.117
           7.937          8.647E
          0.8233E
          0.8233E
              12              1              3              3
               2              1              3              2
R 2          0.0R 3         1.0R 4         0.0E
F            1.00E
          0.1840         0.5460         0.8790         1.0000         0.8790
          0.5460         0.1840E
          1824.0E
             0.0     1.350E-03      2.700E-03      3.000E-03      3.300E-03
       3.825E-03      4.350E-03      4.850E-03      5.350E-03E
R 2            8R 2           5R 2           4R 2           10E
             0.0         9.82E6           10.0          9.35E6           25.0
          8.86E6           45.0          8.41E6           70.0          8.01E6
           101.0          7.66E6           152.0          7.23E6           212.0
          6.71E6           282.0          6.28E6           502.0          5.45E6E
F               1E
F             0.0E
F             0.0E
F             0.0E
F             0.0E
F             0.0E
F             0.0E
F             0.0E
F             0.0E
F            22.00E                                                              LEVEL 1
F           547.60E
F             0.0E
F             0.0E
F             0.0E
F             0.0E
F             0.0E
F             0.0E
F           0.8174E
F           0.0000E
F           0.8174E
F           0.0000E
F           0.0000E
F           0.0278E
F           0.0000E
F            400.2E
F             0.0E
F             0.0E
F             0.0E
F             0.0E
F             0.0E
F             0.0E
```

```
F          0.0E
F        400.2E
F        400.2E
F       4.10E5E
F         22.00E          LEVEL 2
F        547.60E
F          0.0E
F          0.0E
F          0.0E
F          0.0E
F          0.0E
F          0.0E
F        0.8174E
F        0.0000E
F        0.3628E
F        0.0000E
F        0.0000E
F        0.0278E
F        0.0000E
F        400.2E
F          0.0E
F          0.0E
F          0.0E
F          0.0E
F          0.0E
F          0.0E
F        400.2E
F        400.2E
F       4.10E5E
F         30.48E          LEVEL 3
F        532.00E
F          0.0E
F          0.0E
F          0.0E
F          0.0E
F          0.0E
F          0.0E
F        0.7739E
F        0.0000E
F        0.7739E
F        0.0000E
F        0.0000E
F        0.0278E
F        0.0000E
F        405.00E
F          1.0E
F          0.0E
F          0.0E
F          0.0E
F          0.0E
F          0.0E
F          0.0E
F        405.00E
F        405.00E
F       4.10E5E
F         30.48E          LEVEL 4
F        532.00E
F          0.0E
```

```
F          0.0E
F          0.0E
F          0.0E
F          0.0E
F          0.0E
F        0.7739E
F        0.0000E
F        0.0828E
F        0.0000E
F        0.0000E
F        0.0252E
F        0.0000E
F        405.00E
F          1.0E
F          0.0E
F          0.0E
F          0.0E
F          0.0E
F          0.0E
F          0.0E
F          0.0E
F        405.00E
F        405.00E
F       4.10E5E
F          7.88E          LEVEL 5
F        116.24E           CORE #1
F          0.0E
F          0.0E
F          0.0E
F          0.0E
F          0.0E
F          0.0E
F        0.3688E
F        0.0000E
F        0.3688E
F        0.0000E
F        0.0000E
F        0.0163E
F        0.0000E
F        405.00E
F          1.0E
F          0.0E
F          0.0E
F          0.0E
F          0.0E
F          0.0E
F          0.0E
F        405.00E
F        405.00E
F       4.10E5E
F          7.88E          LEVEL 6
F        116.24E           CORE #2
F          0.0E
F          0.0E
F          0.0E
F          0.0E
F          0.0E
F          0.0E
F        0.3688E
F        0.0000E
```

```
F       0.3688E
F       0.0000E
F       0.0000E
F       0.0163E
F       0.0000E
F       405.00E
F          1.0E
F           .0E
F          0.0E
F          0.0E
F          0.0E
F          0.0E
F          0.0E
F       405.00E
F       405.00E
F       4.10E5E
F         7.88E          LEVEL 7
F       116.24E           CORE #3
F          0.0E
F          0.0E
F          0.0E
F          0.0E
F          0.0E
F          0.0E
F       0.3688E
F       0.0000E
F       0.3688E
F       0.0000E
F       0.0000E
F       0.0163E
F       0.0000E
F       405.00E
F          1.0E
F           .0E
F          0.0E
F          0.0E
F          0.0E
F          0.0E
F          0.0E
F       405.00E
F       405.00E
F       4.10E5E
F         7.88E          LEVEL 8
F       116.24E           CORE #4
F          0.0E
F          0.0E
F          0.0E
F          0.0E
F          0.0E
F          0.0E
F       0.3688E
F       0.0000E
F       0.3688E
F       0.0000E
F       0.0000E
F       0.0163E
F       0.0000E
F       405.00E
F          1.0E
```

```
F           .0E
F          0.0E
F          0.0E
F          0.0E
F          0.0E
F          0.0E
F       405.00E
F       405.00E
F       4.10E5E
F         7.88E          LEVEL 9
F       116.24E           CORE #5
F          0.0E
F          0.0E
F          0.0E
F          0.0E
F          0.0E
F          0.0E
F       0.3688E
F       0.0000E
F       0.3688E
F       0.0000E
F       0.0000E
F       0.0163E
F       0.0000E
F       405.00E
F          1.0E
F           .0E
F          0.0E
F          0.0E
F          0.0E
F          0.0E
F          0.0E
F       405.00E
F       405.00E
F       4.10E5E
F         7.88E          LEVEL 10
F       116.24E           CORE #6
F          0.0E
F          0.0E
F          0.0E
F          0.0E
F          0.0E
F          0.0E
F       0.3688E
F       0.0000E
F       0.2639E
F       0.0000E
F       0.0000E
F       0.0163E
F       0.0000E
F       405.00E
F          1.0E
F           .0E
F          0.0E
F          0.0E
F          0.0E
F          0.0E
F          0.0E
F       405.00E
```

```
F       405.00E
F       4.10E5E
F         2.80E         LEVEL 11
F       140.00E          U.P.
F          0.0E
F          0.0E
F          0.0E
F          0.0E
F          0.0E
F          0.0E
F       0.9520E
F       0.0000E
F       0.3414E
F       0.0000E
F       0.0000E
F       0.1225E
F       0.0000E
F       405.00E
F          1.0E
F          0.0E
F          0.0E
F          0.0E
F          0.0E
F          0.0E
F          0.0E
F       405.00E
F       405.00E
F       4.10E5E
F        14.40E         LEVEL 12
F       720.00E          U.P.
F          0.0E
F          0.0E
F          0.0E
F          0.0E
F          0.0E
F          0.0E
F       0.9520E
F       0.0000E
F       0.9442E
F       0.0000E
F       0.0000E
F       0.1225E
F       0.0000E
F       405.00E
F          1.0E
F          0.0E
F          0.0E
F          0.0E
F          0.0E
F          0.0E
F          0.0E
F       405.00E
F       405.00E
F       4.10E5E
F         5.60E         LEVEL 13
F       280.00E          U. P.
F          0.0E
F          0.0E
F          0.0E
```

```
F           0.0E
F           0.0E
F           0.0E
F         0.9520E
F         0.0000E
F         0.0000E
F         0.0000E
F         0.0000E
F         0.1225E
F         0.0000E
F         405.00E
F            1.0E
F            0.0E
F            0.0E
F            0.0E
F            0.0E
F            0.0E
F            0.0E
F            0.0E
F         405.00E
F         405.00E
F         4.10E5E
F            0.0E
R 9       405.0R 9       405.0R 9       405.0R 9       405.0R 9       405.0
R 9       405.0R 9       405.0E
         1.0E-06        2.5E-02          50.0
            20.0           1.0           20.0
         1.0E-06        0.5E-02          90.0
            10.0           0.20          10.0
         1.0E-06        1.0E-02         100.0
            20.0           0.50          20.0
-1.
```